Bioorganic Chemistry 98 (2020) 103735

Contents lists available at ScienceDirect

Bioorganic Chemistry

journal homepage: www.elsevier.com/locate/bioorg

Novel paeonol derivatives: Design, synthesis and anti-inflammatory activity *in vitro* and *in vivo*

Yang Sheng Hu, Xu Han, Pei Jing Yu, Ming Ming Jiao, Xin Hua Liu*, Jing Bo Shi*

School of Pharmacy, Anhui Medical University, Hefei 230032, PR China

ARTICLE INFO

Keywords:
Paeonol derivatives
Nitric oxide
Inhibit
Anti-inflammatory

ABSTRACT

Paeonol has been proved to have potential anti-inflammatory activity, but its clinical application is not extensive due to the poor anti-inflammatory activity (14.74% inhibitory activity at 20 μM). In order to discover novel lead compound with high anti-inflammatory activity, series of paeonol derivatives were designed and synthesized, their anti-inflammatory activities were screened *in vitro* and *in vivo*. Structure-activity relationships (SARs) have been fully concluded, and finally (*E*)-*N*-(4-(2-acetyl-5-methoxyphenoxy)phenyl)-3-(3,4,5-trimet-hoxyphenyl) acrylamide (compound **11a)** was found to be the best active compound with low toxicity, which showed 96.32% inhibitory activity at 20 μM and IC_{50} value of 6.96 μM against LPS-induced over expression of nitric oxide (NO) in RAW 264.7 macrophages. Preliminary mechanism studies indicated that it could inhibit the expression of TLR4, resulting in inhibiting of NF-κB and MAPK pathways. Further studies have shown that compound **11a** has obvious therapeutic effect against the adjuvant-induced rat arthritis model.

1. Introduction

Paeonol, 1-(2-hydroxy-4-methoxyphenyl)ethan-1-one, the major phenolic component of moutan cortex radicis, has been used as an anti-inflammatory drug in China [1,2]. In addition, paeonol has also been found to have other biological effects, such as antitumor [3,4], anti-hepatitis B virus [5], antibacterial [6], antidiabetic [7] and antioxidant [8] activity. Currently, paeonol has been used clinically as an anti-inflammatory drug approved by the CFDA (China Food and Drug Administration), including various dosage forms, tablet, ointment, adhesive and injection [2]. However, paeonol was not widely known in the treatment of inflammatory diseases compared to other anti-inflammatory drugs in China, such as indometacin, celecoxib, asprin, etc. Among various dosage forms, paeonol ointment is used for the treatment of dermatitis. In order to expand paeonol use, we focus on this moiety. Preliminary experimental studies show its anti-inflammatory activity is extremely poor (14.74% inhibitory activity at 20 μM). Herein, to improve its anti-inflammatory activity, it is of significance to design and synthesize novel efficient paeonol-based derivatives. As a classic drug design method, fragment-based drug design (FBDD) is one of the way to obtain highly active compounds [9]. Based on paeonol moiety, through structural optimizations (see *2.1 Design and 2.5* Structure-activity relationships), we will describe our efforts toward the discovery of novel paeonol derivatives with high anti-inflammatory activity.

Rheumatoid arthritis (RA) is an autoimmune disease, which is characterized by chronic progressive inflammatory disease of joints and surrounding tissues, eventually leads to irreversible joint damage [10]. It is widely accepted that the change of inflammatory cytokines concentration is related to the occurrence of RA [11]. More and more evidence show that the content of pro-inflammatory factors in serum and synovial fluid of RA patients is very high [12]. A large number of inflammatory factors promote the entry of inflammatory cells into tissues, aggravating the destruction of joints, which eventually leads to the occurrence of arthritis [13]. At present, the conventional therapy and biological therapy can only partially relieve RA [14]. For most patients, there is still an urgent need to discover new drugs. It has been reported that paeonol can trigger innate immune system by affecting TLR4, and then inhibit the release of pro-inflammatory cytokines induced by nuclear factor (NF-κB) and mitogen activated protein kinase (MAPK) [15–17]. Meanwhile, paeonol can reverse the excessive production of inducible nitric oxide synthase (iNOS) [18].

2. Results and discussion

2.1. Design

Huang et al. [19] etherified 2-hydroxyl group of paeonol with long-

* Corresponding authors.
E-mail addresses: xhliuhx@163.com (X.H. Liu), sjbo616@126.com (J.B. Shi).

https://doi.org/10.1016/j.bioorg.2020.103735
Received 17 January 2020; Received in revised form 17 February 2020; Accepted 6 March 2020
Available online 08 March 2020

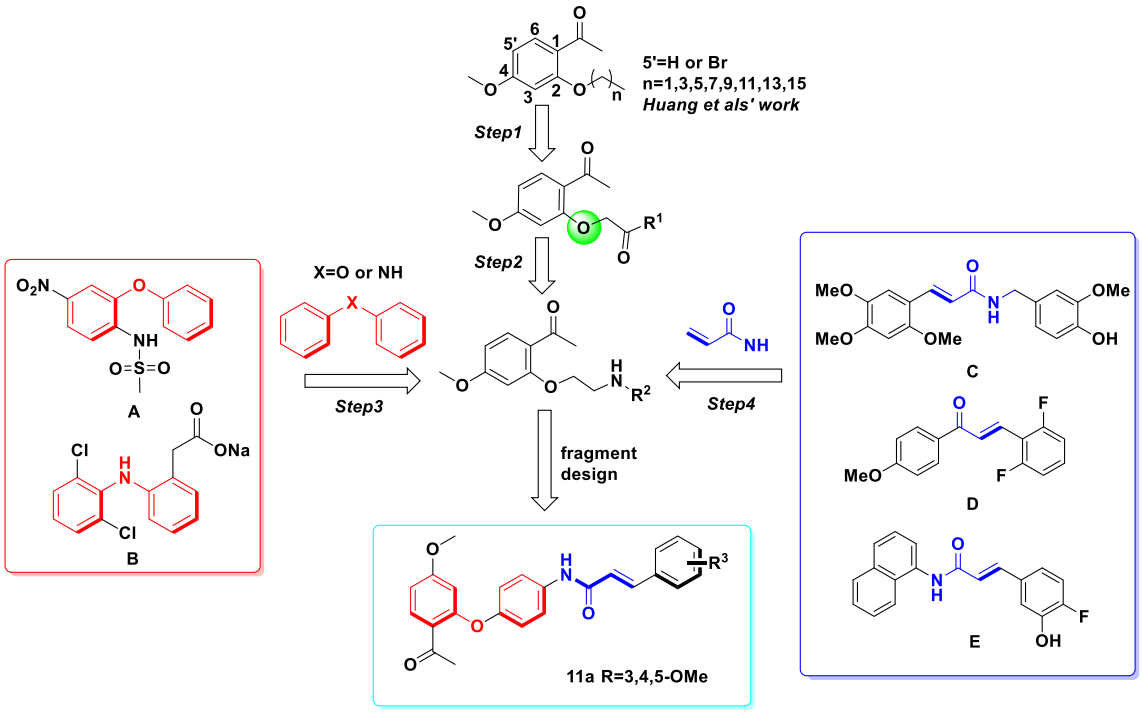

Fig. 1. The process of design and analysis. Nimesulide (**A**) and diclofenac acid (**B**) contain a two-benzene ring scaffold linked by O or NH (red section) α, β-unsaturated amide structure including compound **C**, **D**, **E** (blue section). (For interpretation of the references to colour in this figure legend, the reader is referred to the web version of this article.)

chain fatty alkane and found that some alkyl ether analogues of bromopaeonol could improve the anti-inflammatory activity. In order to observe whether the aromatic system has an effect on the activity, we introduced a benzene ring through a short linker and performed a two-step optimization (step 1, step 2) at first (Fig. 1).

Among the many non-steroidal anti-inflammatory drugs, both nimesulide (**A**) [20] and diclofenac acid (**B**) [21] were found to have a two-benzene ring scaffold linked by O or NH, and therefore similar structural fragments were introduced to paeonol moiety (step 3) in this study. On the other hand, α, β-unsaturated ketone and unsaturated amide moieties have been the common scaffolds with various biological activities [22], So, on the basis of this and the summative SARs (**C**, **D**, **E**), the final step (step 4) was carried out by adding α, β-unsaturated moiety.

2.2. Chemistry

The routes to synthesize the final compounds were depicted in Scheme 1. Through a simple nucleophilic substitution, intermediates **1** and **4** were synthesized. The intermediate **1** was hydrolyzed, acidified, and amidated to obtain the final compounds **3a-3l**. The intermediate **4** was amidated to get the final compounds **6a-6m**. Reaction of paeonol with *p*-nitrofluorobenzene get intermediate **8** with high yield [23], then nitro group is reduced with Pd/C as catalyst under H_2 atmosphere to obtain intermediate **9**. Oxalyl chloride activates carboxylic acid to acyl chloride intermediate, Intermediate **9** was subjected to the condensation to give compounds **10a-10e**, **11a-11e**. The detailed synthesis procedures were listed in experimental section.

2.3. Assessment of toxicity of active compounds

Before the determination of the anti-inflammatory activity in LPS-induced RAW 264.7 cells, compounds' cytotoxicity against RAW 264.7 cells was tested by MTT assay. As shown in Fig. 2. All compounds exhibited no obvious toxicity against cell proliferation at 20 μM.

2.4. NO release in RAW 264.7

It has been demonstrated that NO is well-known pro-inflammatory mediator [24]. It has been found that excessive NO production plays an important role in many inflammatory diseases [25]. The stimulation of macrophages with LPS produces overexpressed pro-inflammatory cytokines and pro-inflammatory mediators [26]. Here, all compounds were examined their ability of inhibiting over expression NO. RAW 264.7 cells were pre-incubated with the compounds (20 μM) for 1 h, then treated with LPS (0.5 μg/mL) for 24 h. Determination of NO concentration in cell supernatant by Griess reagent. The results showed that most of paeonol derivatives effectively suppressed LPS-induced NO release in *vitro* (Tables 1–5). Most of compounds have improved inhibitory activity compared to paeonol at 20 μM. In particularly, compound **11a** exhibited the most potent activity with IC_{50} value of 6.96 μM (Fig. 3).

2.5. Structure-activity relationships (SARs)

Firstly, compounds **3a-3l** and their inhibitory rates (IR) were listed in Table 1. Most of compounds showed weak inhibitory activity against LPS-induced NO production at 20 μM (IRs were less than 23.33%). Compared to paeonol, its derivatives had better anti-inflammatory activity through introduction of aromatic system. On basis of this, in order to improve the anti-inflammatory activity, we continued to optimize them. As shown in Table 2, acetamide linker was replaced with ethylamine and the order of amide was reversed, compounds **6a-6m** were designed and synthesized. The anti-inflammatory effect of these compounds was greatly improved, especially compounds **6d**, **6i** with 75.94% and 63.29% inhibitory activity at 20 μM, respectively. From Tables 1 and 2, it is easy to found that the anti-inflammatory activity should be improved when the strong electron withdrawing group was substituted on the aromatic ring, such as $-CF_3$ (compounds **3b** and **6d**), $-OCH_3$ (compounds **3g** and **6c**), −F (compounds **3i** and **6i**).

As we mention in the design section, fragment design was used for further structural optimization. We initially designed, synthesized

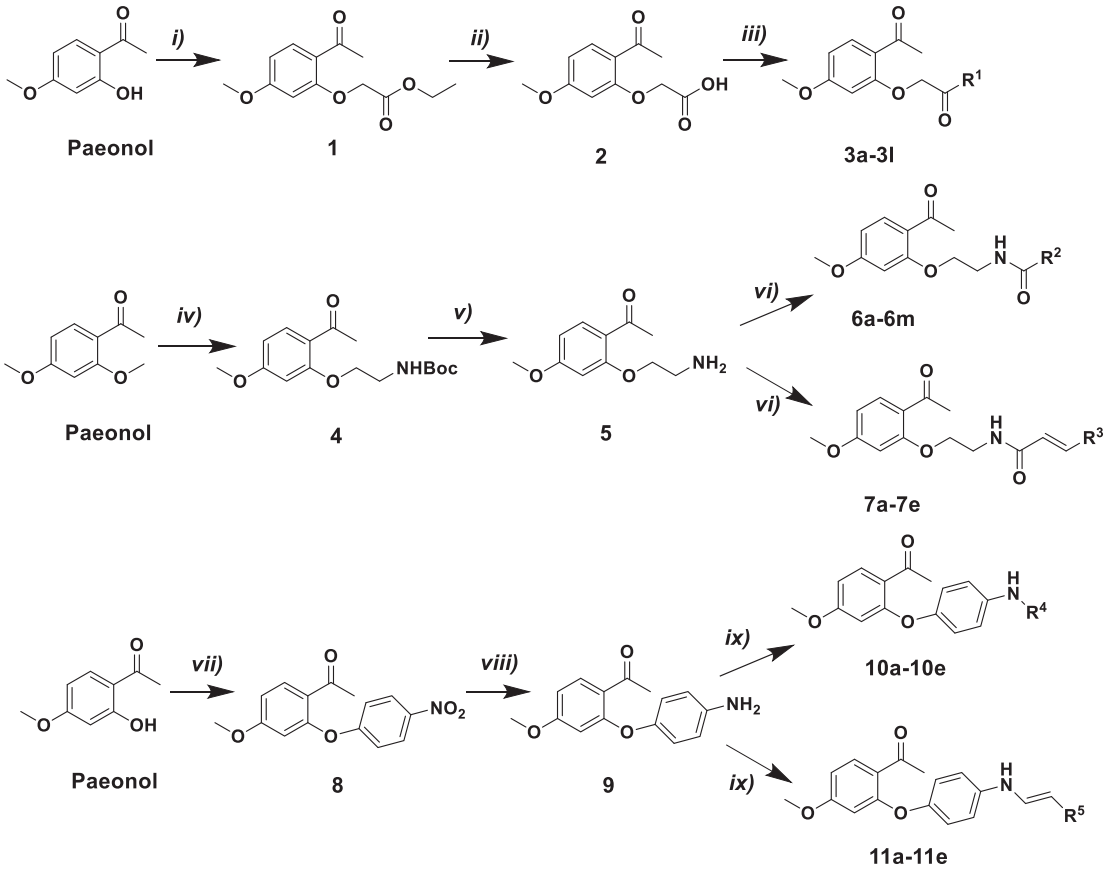

Scheme 1. Synthesis of title compounds, **Reagents and conditions**: (***i***) ethyl bromoacetate, K_2CO_3, acetone, rt; (***ii***) (1) 5% NaOH aq: ethanol (1:1), 65 °C. (2) 1 N HCl, pH 3–4, rt; (***iii***) R-NH_2 or 1-methylpiperazine or morpholine, HOBT, EDCI, Et_3N, Dichloromethane, rt; (***iv***) *tert*-butyl (2-bromoethyl)carbamate, K_2CO_3, DMF, 80 °C; (***v***) HCl: ethanol (1:1), rt; (***vi***) R-COOH, HOBT, EDCI, Et_3N, Dichloromethane, rt; (***vii***) 4-fluoronitrobenzene, K_2CO_3, DMSO, rt; (***viii***) H_2, Pd/C, methanol, rt; (***ix***) (1) R-COOH, oxalyl chloride, DMF (cat), Dichloromethane, rt. (2) compound **9**, Et_3N, Dichloromethane, 0 °C ~ rt.

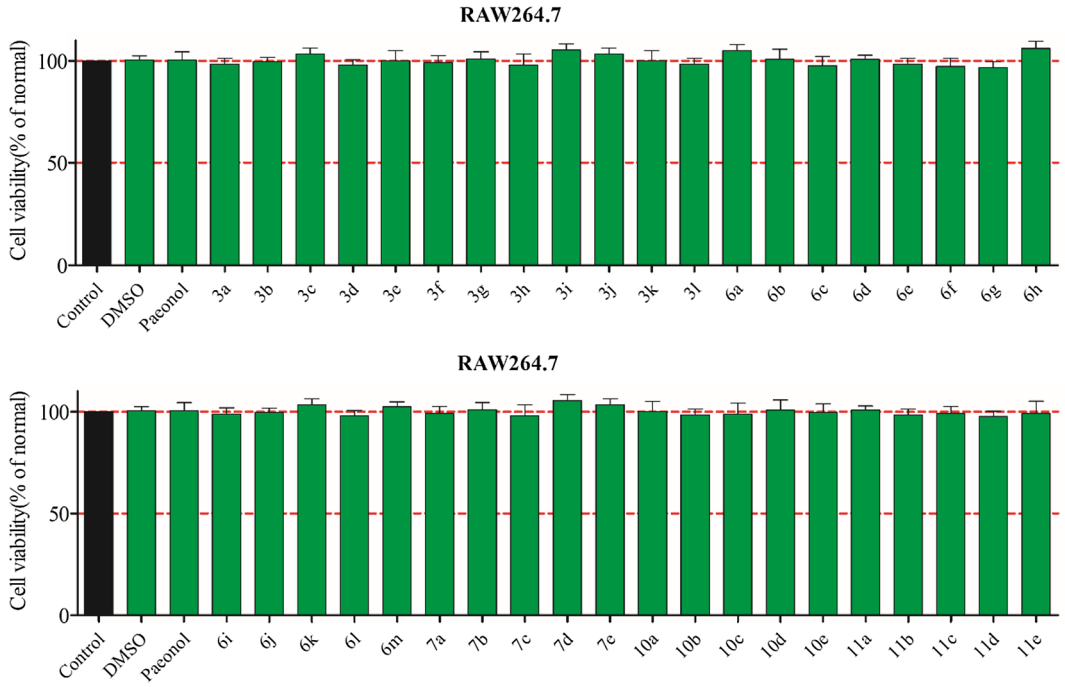

Fig. 2. Cytotoxic evaluation of all compounds, the cytotoxic evaluation of compounds **3a-3l**, **6a-6m**, **7a-7e**, **10a-10e** and **11a-11e** in RAW264.7 cells. Compounds at concentration of 20 μM. Paeonol at concentration of 20 μM. The concentration of DMSO is 10^{-8} μM. Control: Untreated cells. The cell viability was evaluated by the MTT assay. ***$p < 0.001$ compare with control group.

Table 1

Inhibitory activity against NO production of compounds **3a-3l**.

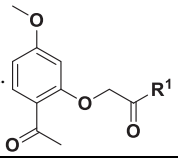

Compd	R^1	Inhibition rate (20 μM)	Compd	R^1	Inhibition rate (20 μM)
3a	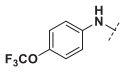	18.33 ± 10.21	**3h**	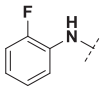	3.37 ± 6.38
3b	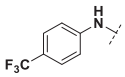	23.33 ± 5.21	**3i**	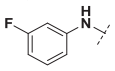	20.22 ± 14.23
3c	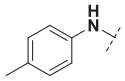	6.74 ± 12.11	**3j**	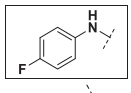	21.67 ± 7.23
3d	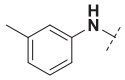	5.32 ± 10.21	**3k**	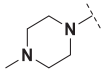	17.98 ± 10.23
3e	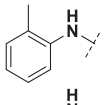	21.66 ± 10.32	**3l**		19.10 ± 10.20
3f	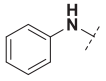	7.86 ± 10.45	**Paeonol**	–	14.74 ± 5.62
3g	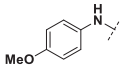	20.22 ± 8.96			

compounds (**7a-7e**, **10a-10e**) as shown in Tables 3 and 4. And the difference is that one is two-benzene ring scaffold linked by O atom and the other is α, β-unsaturated ketone structure. The anti-inflammatory activity results demonstrated that compounds with two-benzene ring scaffold linked by O atom had a slight increase, but, compounds' activity containing α, β-unsaturated ketone moiety was greatly improved. Finally, we then tried to combine two-benzene ring scaffold and α, β-unsaturated amide together to get compounds **11a-11e** as shown in Table 5. To our delight, the anti-inflammatory activity of these derivatives has been greatly improved again. Among them, the IR of compound **11a** against NO reached 96.32%. Therefore, after several rounds of optimization, lead compound **11a** was initially selected for further mechanism research.

2.6. Compound *11a* suppresses LPS-induced iNOS and COX-2 activation

iNOS and COX-2 are well-known pro-inflammatory proteins [27,28]. Many inflammatory diseases can active related cellular pathways and lead to high expressions of iNOS and COX-2. Therefore, inhibition of excessive expression of iNOS and COX-2 can attenuate the

Table 2

Inhibitory activity against NO production of compounds **6a-6m**.

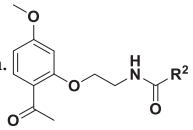

Compd	R^2	Inhibition rate (20 μM)	Compd	R^2	Inhibition rate (20 μM)
6a		32.12 ± 5.62	**6h**		48.10 ± 9.22
6b	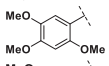	31.64 ± 6.21	**6i**		63.29 ± 8.22
6c	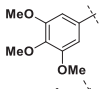	48.10 ± 5.32	**6j**		27.84 ± 3.56
6d		75.94 ± 8.23	**6k**		26.13 ± 2.33
6e		45.57 ± 6.23	**6l**		18.98 ± 10.23
6f		31.64 ± 3.20	**6m**		36.71 ± 4.25
6g	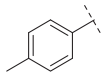	60.75 ± 10.24	**Paeonol**	–	14.74 ± 5.62

Table 3
Inhibitory activity against NO production of compounds **10a-10e**.

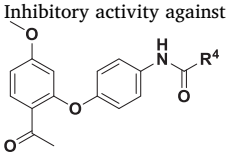

Compd	R^4	Inhibition rate (20 μM)
10a	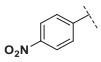	38.20 ± 5.62
10b	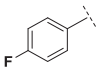	28.10 ± 3.23
10c	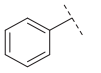	25.84 ± 4.15
10d	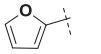	20.22 ± 6.32
10e	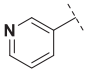	15.50 ± 6.33
Paeonol	–	14.74 ± 5.62

Table 4
Inhibitory activity against NO production of compounds **7a-7e**.

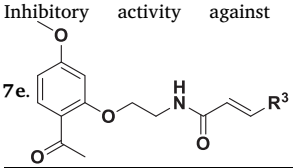

Compd	R^3	Inhibition rate (20 μM)
7a	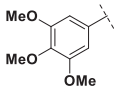	88.76 ± 3.25
7b	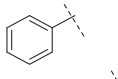	32.58 ± 5.62
7c	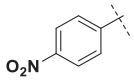	44.94 ± 6.23
7d	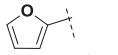	57.30 ± 2.15
7e	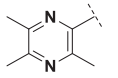	17.98 ± 4.25
Paeonol	–	14.74 ± 5.62

severity of inflammatory diseases [28]. In the present study, compound **11a** significantly suppressed LPS-induced protein expression, and it could markedly augmente expressions of iNOS and COX-2 (Fig. 4). The results indicated that compound **11a** could prevent LPS induced inflammatory response in macrophages.

2.7. Compound *11a* inhibits LPS-induced NF-κB signaling pathways activation

Accumulated data indicate that NF-κB transcription factor is one of the principal factors for protein expression and cytokines secretion mediated by LPS [29]. Transcription factor p65, which is one member of NF-κB family, plays the most important role in signaling pathway. In the control cells, NF-κB is inactivated in the cytoplasm by binding to IκB. When a large number of inflammatory cytokines (such as LPS and TNF-α) stimulate cells, IκB kinase (IKK) can be activated and then cause IκB phosphorylation and degradation. At last, NF-κB enters the nucleus and binds with the target gene to promote transcription and translation

Table 5
Inhibitory activity against NO production of compounds **11a-11e**.

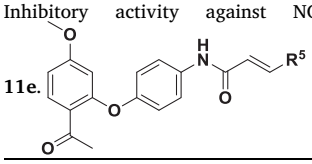

Compd	R^5	Inhibition rate (20 μM)
11a	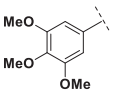	96.32 ± 5.32
11b		89.66 ± 3.12
11c	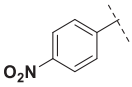	28.73 ± 5.63
11d		94.38 ± 6.32
11e	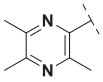	56.32 ± 8.23
Paeonol	–	14.74 ± 5.62

[30].

Thus, we examined whether compound **11a** inhibited phosphorylation and degradation of IκB. RAW 264.7 cells were pretreated with different concentration for 1 h and then treated with 0.5 mg/mL LPS for 30 min. The results showed that compound **11a** significantly suppressed LPS-induced phosphorylation and degradation of IκB. We further examined the nuclear translocation of P65 by Western blot. We found that compound **11a** significantly suppressed LPS-induced P65 phosphorylation (Fig. 5). These results suggested that **11a** might inhibit NF-κB activation by blocking the LPS-induced phosphorylation of IκB and P65.

2.8. Compound *11a* inhibits LPS-induced ERK and P38 signaling activation

TLR4 is a member of the TLR family that is involved in innate immunity and inflammation response [31]. TLR4 is traditionally accepted as the primary LPS receptor and has been reported as critical for the inflammatory response to LPS [32]. The TLR4 mediated signaling plays an important role in the activation of NF-κB and MAPK signaling in LPS-induced macrophages [29]. When LPS stimulates cells, the NF-κB and MAPK are activated through TIR4-MyD88-TAK1-dependent signaling pathways, and then inflammatory cytokines and inflammatory proteins are induced. TLR4 is an important upstream factor of the NF-κB and MAPK signaling. Recent studies found that the inhibition of TLR4 protein expression could suppress inflammation [27]. Therefore, we studied whether compound **11a** inhibited TLR4 expression by Western blot. The results showed that TLR4 was up-regulated in LPS induced RAW264.7 cells, and the expression of TLR4 was reversed in a concentration dependent manner by pretreatment with compound **11a** (Fig. 6A).

MAPKs are also known to participate in regulating inflammation process. MAPK family is mainly composed of ERK, P38 and JNK subfamily. When LPS-stimulated macrophages induce inflammation, MAPKs protein will be phosphorylated, which will increase the translocation of the transcription factor AP-1 into the nucleus and bind to the target promoter, thereby turning on the transcription of inflammatory genes. Therefore, we detected the effect of compound **11a** in MAPK signaling pathway by Western blots. The results suggest that the anti-inflammatory effect of compound **11a** was mediated by blockade of ERK and P38 phosphorylation signaling, but not JNK phosphorylation signaling in LPS-induced RAW264.7 cells (Fig. 6B).

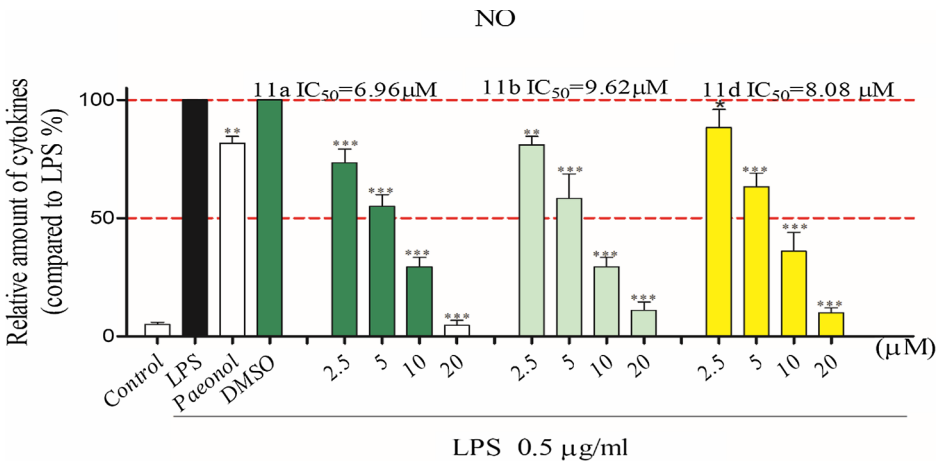

Fig. 3. Inhibitory activity against NO production of compounds **11a**, **11b**, **11d,** RAW264.7 cells were pretreated with compounds (20, 10, 5, 2.5 μM) for 1 h, incubated with LPS (0.5 μg/mL) for 24 h, NO production was measured using Griess Reagent assay. Paeonol (20 μM) is a positive compound. The concentration of DMSO is 10^{-8} μM ***p < 0.001, **p < 0.01, *p < 0.05 *vs* LPS group.

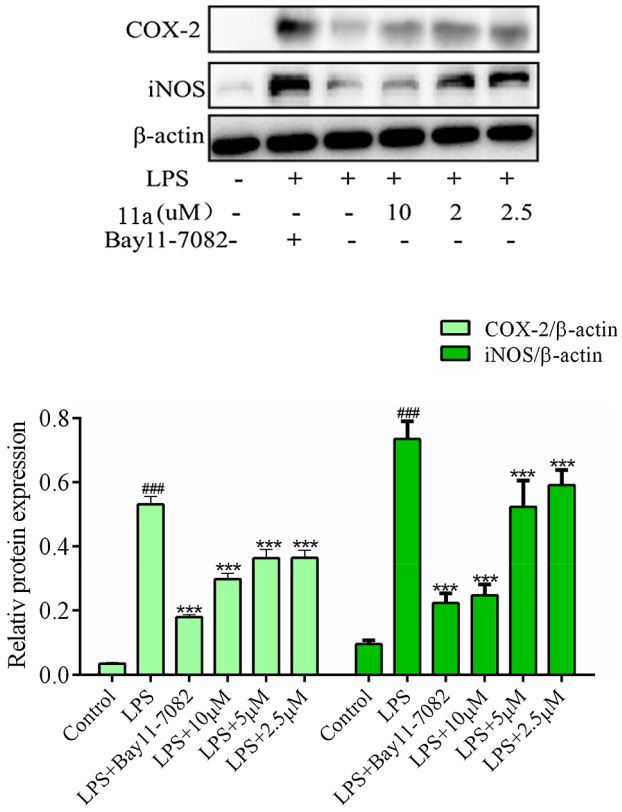

Fig. 4. Compound **11a** inhibited the LPS-induced expression of iNOS and COX-2 in RAW 264.7 cells, Cells were pre-treated with compound **11a** at concentration of 10, 5 and 2.5 μM for 1 h, then stimulated with LPS (0.5 μg/mL) for 30 min. Bay 11–7082 (5 μM) is the NF-κB inhibitor. ###p < 0.001 compared with LPS unstimulated cells, ***p < 0.001, compared with LPS-stimulated cells; the blots shown are the examples of three separate experiments.

*2.9. In vivo activity of compound **11a***

Rheumatoid arthritis (RA) is a chronic inflammatory autoimmune disease characterized by joint swelling, synovitis, and progressive joint injury of cartilage and bone. The complete Freund's adjuvant (CFA)-induced arthritis (AA) is widely used in the study of RA because of its similar pathogenesis. Complete Freund's adjuvant consists of incomplete Freund's adjuvant and inactivated BCG vaccine (10 mg/mL). Rat was induced by a single intradermal injection of 0.1 mL CFA into the right hind paw. We observed that 70–80% of rats exhibited obvious left hind pawhind paw swelling and body weight loss. Rats were given intragastric administration of compound **11a** once a day from day 14 to 28. Sinomenine was given intragastrically as the positive control.

In order to evaluate the in *vivo* effect of compound **11a**, histopathological analysis of the ankle joint was performed at the end of the experiment. There was no inflammatory reaction in normal rats, and the articular cavity was intact without any inflammatory cells (Fig. 7A). AA rats exhibited extensive inflammation, inflammatory cells infiltration, synovial hyperplasia and bone or cartilage destruction (Fig. 7B). AA rats treated with compound **11a** (40 mg/kg) exhibited moderate synovial hyperplasia, inflammatory cells infiltration and cartilage destruction (Fig. 7D). Compound **11a** (80 mg/kg) and sinomenine (80 mg/kg) ameliorated cartilage destruction and severe inflammatory cell infiltration (Fig. 7C, E). Although sinomenine showed moderate synovial hyperplasia, the articular cavity is intact. Compound **11a** (80 mg/kg) showed slightly synovial hyperplasia. In conclusion, the results of histopathological evaluation showed that compound **11a** had anti-inflammatory effect on AA rats.

3. Conclusions

In summary, total of 40 new compounds were synthesized, characterized and evaluated for their anti-inflammatory activities. After several rounds SARs step by step, title compound **11a** was discovered as the most potent compound without obvious cytotoxicity. The preliminary mechanism indicated that this compound could significantly suppress LPS-induced expressions of iNOS, COX-2 and inhibit NO production through NF-κB/MAPK signaling pathway in a concentration dependent manner (Fig. 8). The further in *vivo* anti-inflammatory study revealed that this compound effectively relieved the histological changes in knee joints of AA rats. Therefore, this title compound is of importance in the development of more efficient agents against anti-AA in the future.

4. Experimental section

4.1. Chemistry

All reagents and solvents were purchased from commercial suppliers and used without further purification. Reactions were monitored by thin-layer chromatography (TLC). ^{1}H and ^{13}C NMR spectral data were recorded with a Bruker or Agilent, 400, 600 MHz spectrometer in $CDCl_3$ or DMSO-d_6 using tetramethylsilane (TMS) as the internal standard. High-resolution mass spectrometry (HRMS) was recorded on an Agilent Technologies LC-TOF instrument. The purities of compound **11a** were determined by monitoring at 300 nm and were confirmed to be more than 95% (*Supporting Information*).

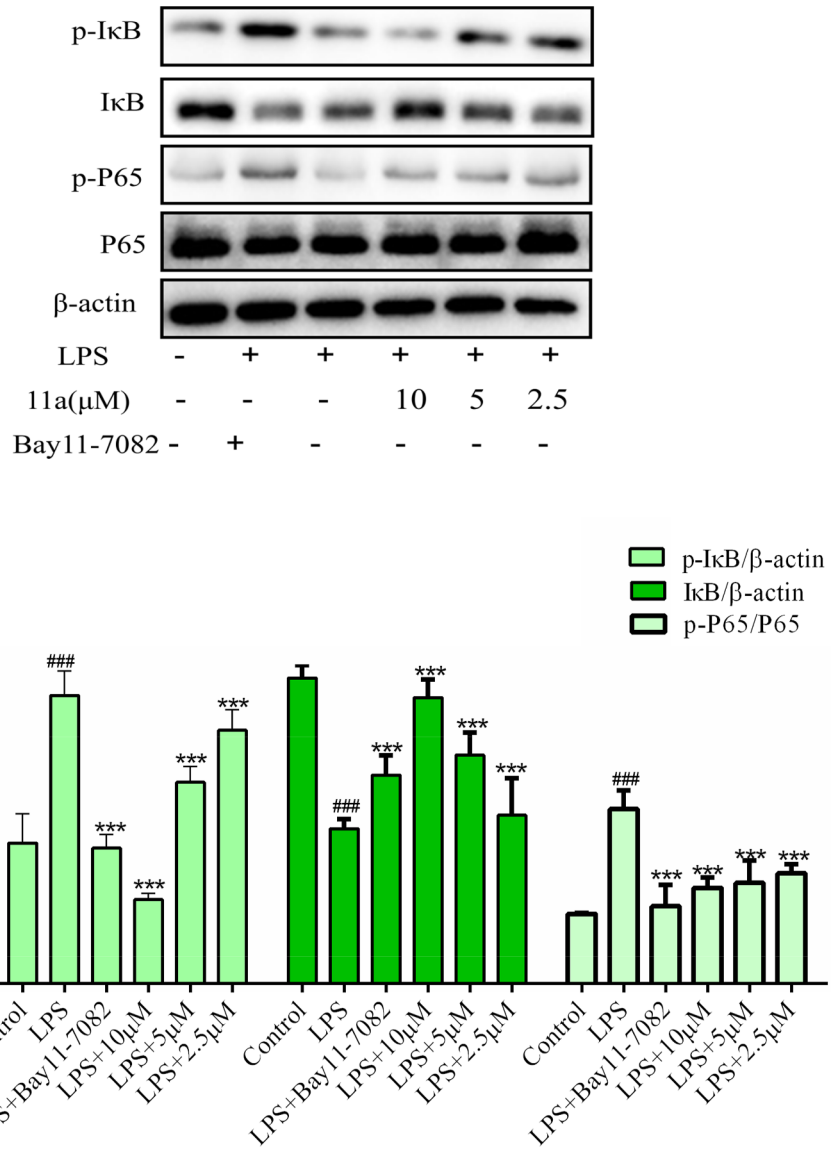

Fig. 5. Compound **11a** inhibited LPS-induced activation of NF-κB signaling pathway in RAW 264.7 cells. After pretreatment with compound **11a** at concentration of 10, 5 and 2.5 μM for 1 h, cells were stimulated with LPS (0.5 μg/mL) for 30 min. Bay 11–7082 (5 μM) is the NF-κB inhibitor. $^{###}p < 0.001$ compared with LPS unstimulated cells, $^{***}p < 0.001$, compared with LPS-stimulated cells.

4.2. The detailed synthesis procedures

*4.2.1. General procedure for synthesis of compounds **3a-3l***

K_2CO_3 (2.5 g, 18 mmol) was added to solution of paeonol (2 g, 12 mmol) in acetone (30 mL). Ethyl bromoacetate (6 g, 36 mmol) was added dropwise. After the reaction was complete, as indicated by TLC, the solvent was removed by rotary evaporation. Crude product was dissolved in ethyl acetate (100 mL), then washed with water and brine (100 mL). The organic layer was dried over anhydrous sodium sulfate, filtered, and the filtrate concentrated under reduced pressure. Residue was recrystallized with ethanol to obtain intermediate **1** as white crystalline solid (2.8 g, yield 92%).

Intermediate **1** (1 g, 4 mmol) was dissolved in 5% NaOH aq/ethanol (1:1, 30 mL) and stirred at 65 °C for 6 h. The mixture was acidified with 1 N HCl to pH 3–4. The precipitate was filtered, washed with water, and dried to give intermediate **2** as white solid (800 mg, yield 90%).

Intermediate **2** (100 mg, 0.446 mmol), 4-(trifluoromethoxy)aniline (79 mg, 0.446 mmol) was dissolved in dichloromethane (5 mL). HOBT (90 mg, 0.669 mmol), EDCI (128 mg, 0.669 mmol) and Et_3N (215 μL, 1.338 mmol) were added at room temperature. The reaction mixture was stirred for overnight. After completion of the reaction, as indicated by TLC, the solvent was removed by rotary evaporation. Residue was purified by flash chromatography to gave compound **3a** (106 mg, 0.227 mmol, 62.17% yield) as white solid. ^{1}H NMR (600 MHz, DMSO-d_6) δ 10.51 (s, 1H), 7.83–7.75 (m, 3H), 7.37 (d, J = 8.6 Hz, 2H), 6.67 (d, J = 8.0 Hz, 2H), 4.88 (s, 2H), 3.83 (s, 3H), 2.60 (s, 3H). ^{13}C NMR (151 MHz, DMSO-d_6) δ 197.46, 166.79, 164.64, 159.46, 144.40, 137.95, 133.06, 122.17(2C), 121.17(2C), 120.80, 120.58 (d, $J_{C\text{-}F}$ = 255.7 Hz), 107.14, 100.39, 68.23, 56.15, 31.32. HRMS (ESI): *m/z* $[M+Na]^+$ calcd for $C_{18}H_{16}F_3NO_5Na$: 406.0873; found: 406.0877.

Following the similar procedures as for compound **3a** gave compounds **3b-3l**.

*4.2.1.1. 2-(2-acetyl-5-methoxyphenoxy)-N-(4-(trifluoromethyl)phenyl) acetamide **(3b)***. White solid, 46.15% yield, m. p.:175–176 °C, ^{1}H NMR (600 MHz, DMSO-d_6) δ 10.66 (s, 1H), 7.90 (d, J = 8.4 Hz, 2H), 7.78 (d, J = 8.4 Hz, 1H), 7.73 (d, J = 8.5 Hz, 2H), 6.67 (d, J = 8.3 Hz, 2H), 4.92 (s, 2H), 3.83 (s, 3H), 2.60 (s, 3H). ^{13}C NMR (151 MHz, DMSO-d_6) δ 197.48, 167.23, 164.64, 159.43, 142.33, 133.07, 126.67 (d, $J_{C\text{-}F}$ = 3.8 Hz, 2C), 124.01 (d, $J_{C\text{-}F}$ = 47.4 Hz), 125.65, 120.78, 119.70

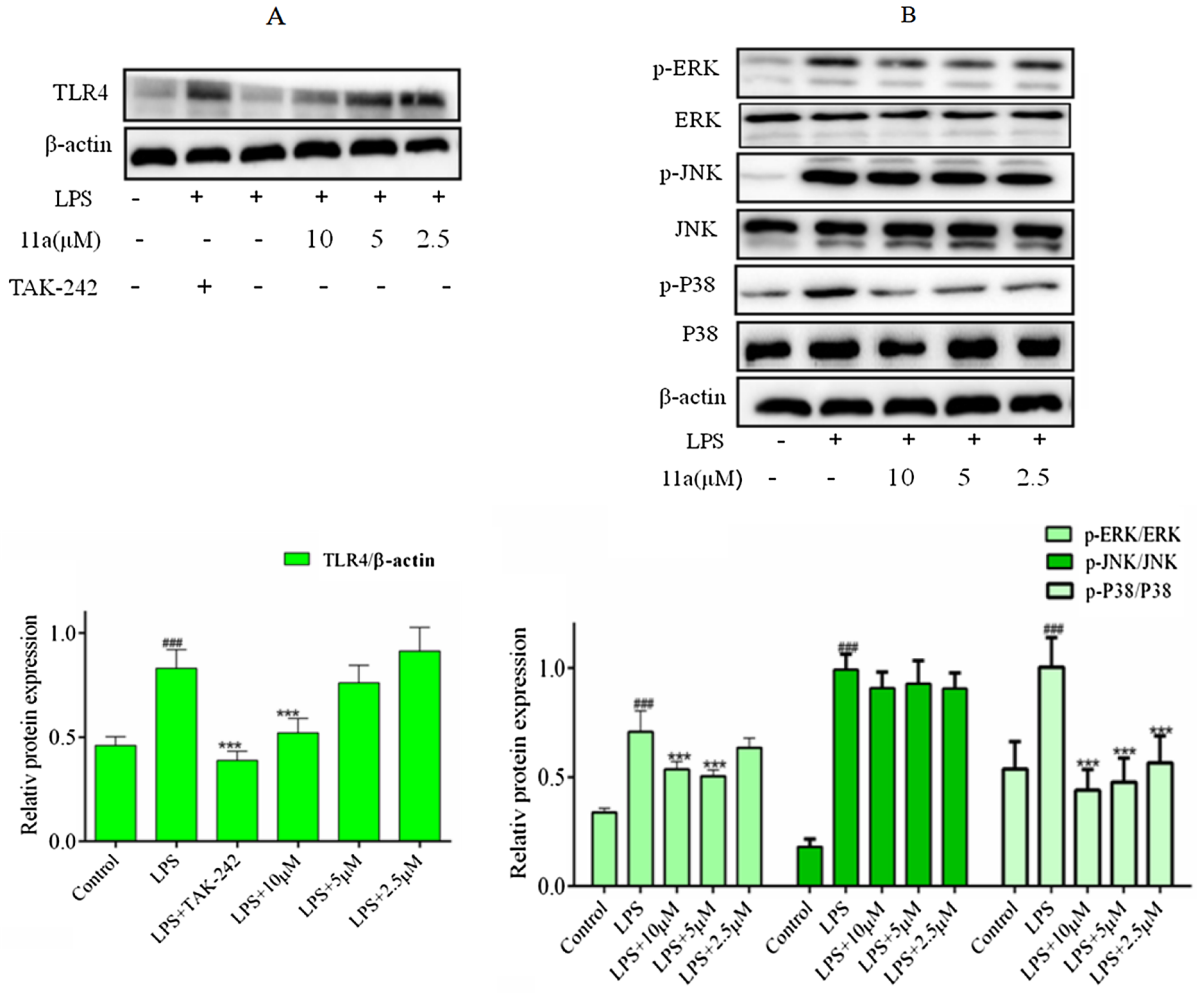

Fig. 6. Compound **11a** dose-dependently suppressed LPS-induced P38 and ERK activation. (**A**) Cells were pre-treated with compound **11a** (10, 5, 2.5 μM) for 1 h, then stimulated with LPS (0.5 μg/mL) for 24 h. TAK-242 (1 μM) is the TLR4 inhibitor. (**B**) Cells were treated with LPS (0.5 μg/mL) for 30 min. The expression of phosphor and total proteins ERK, JNK and P38 were analyzed by Western blot. The results were showed as means ± SD (n = 3) of at least three independent experiments. $^{###}p < 0.001$ compared with LPS unstimulated cells; $^{***}p < 0.001$ compare with LPS-stimulated cells.

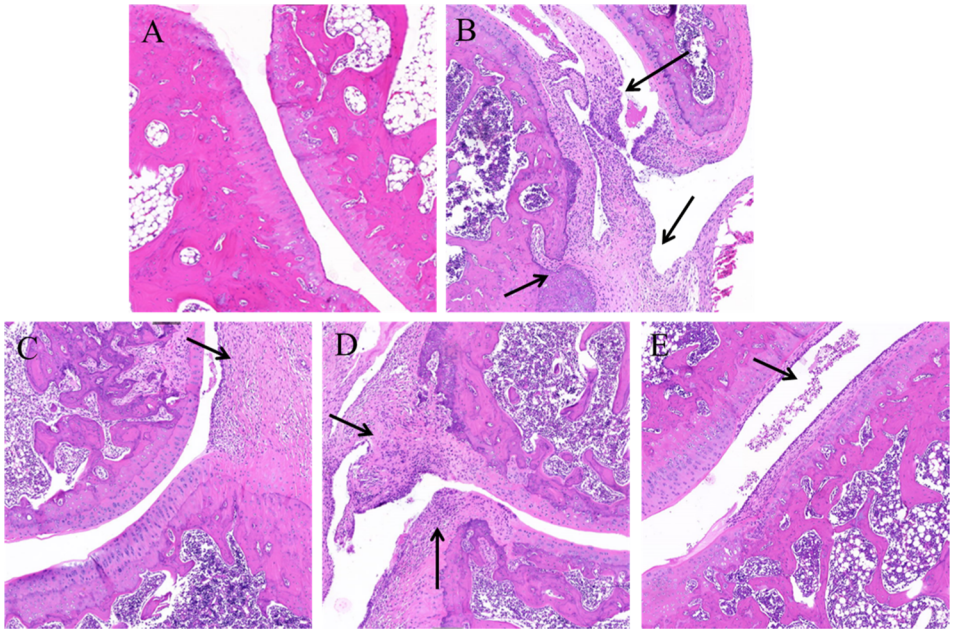

Fig. 7. Therapeutic effect of compound **11a** on AA rats, (**A**) normal; (**B**) AA; (**C**) Sinomenine, 80 mg/kg; (**D**) compound **11a**, 40 mg/kg; (**E**) compound **11a**, 80 mg/kg. Sinomenine was the positive control. Arrows indicate severe inflammatory sites.

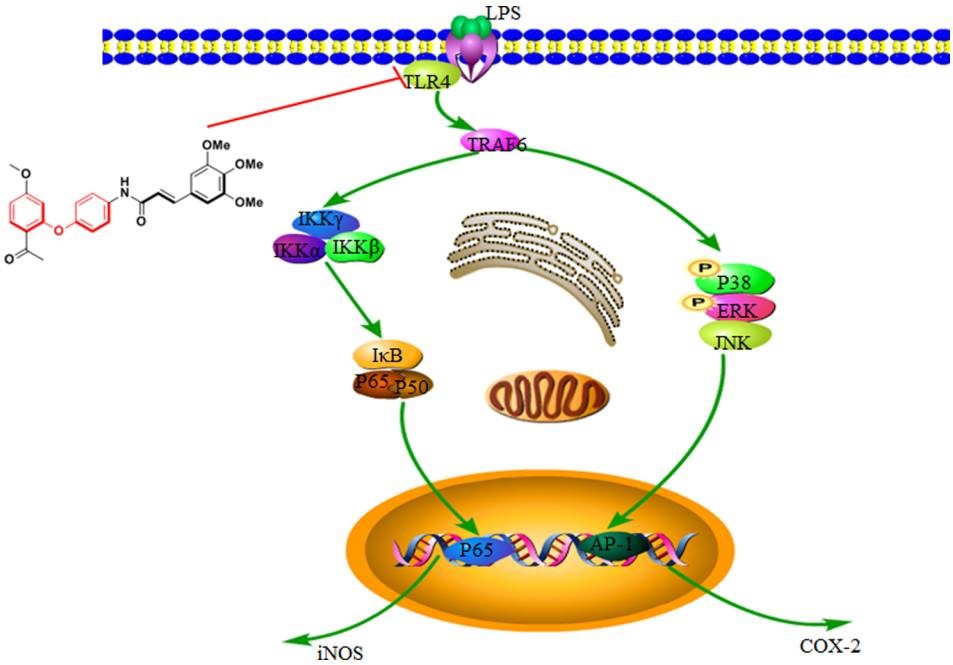

Fig. 8. The possible anti-inflammatory mechanism of compound **11a.**

(2C), 107.15, 100.39, 68.22, 56.16, 31.34. HRMS (ESI): *m/z* $[M+Na]^+$ calcd for $C_{18}H_{16}F_3NO_4Na$: 390.0924; found: 390.0927.

4.2.1.2. 2-(2-acetyl-5-methoxyphenoxy)-N-(p-tolyl)acetamide ***(3c)***. White solid, 58.82% yield, m. p.:159–160 °C, ^{1}H NMR (600 MHz, DMSO-d_6) δ 10.18 (s, 1H), 7.78 (dd, J = 9.3, 4.2 Hz, 1H), 7.59–7.53 (m, 2H), 7.15 (d, J = 8.0 Hz, 2H), 6.66 (dq, J = 4.1, 2.3 Hz, 2H), 4.83 (d, J = 3.6 Hz, 2H), 3.83 (d, J = 3.7 Hz, 3H), 2.59 (d, J = 3.7 Hz, 3H), 2.26 (d, J = 3.6 Hz, 3H). ^{13}C NMR (151 MHz, DMSO-d_6) δ 197.40, 166.23, 164.61, 159.48, 136.26, 133.17, 133.08, 129.67(2C), 120.73, 119.74(2C), 107.06, 100.35, 68.26, 56.14, 31.26, 20.88. HRMS (ESI): *m/z* $[M+Na]^+$ calcd for $C_{18}H_{19}NO_4Na$: 336.1206; found: 336.1209.

4.2.1.3. 2-(2-acetyl-5-methoxyphenoxy)-N-(m-tolyl)acetamide ***(3d)***. White solid, 38.18% yield, m. p.:131–132 °C, ^{1}H NMR (600 MHz, DMSO-d_6) δ 10.21 (s, 1H), 7.82–7.73 (m, 1H), 7.54 (s, 1H), 7.48–7.41 (m, 1H), 7.23 (t, J = 7.8 Hz, 1H), 6.92 (d, J = 7.5 Hz, 1H), 6.67 (d, J = 7.6 Hz, 2H), 4.85 (s, 2H), 3.83 (s, 3H), 2.60 (s, 3H), 2.30 (s, 3H). ^{13}C NMR (151 MHz, DMSO-d_6) δ 197.38, 166.39, 164.60, 159.47, 138.70, 138.54, 133.05, 129.12, 124.90, 120.78, 120.27, 116.97, 107.07, 100.34, 68.25, 56.15, 31.29, 21.61. HRMS (ESI): *m/z* $[M+Na]^+$ calcd for $C_{18}H_{19}NO_4Na$: 336.1206; found: 336.1208.

4.2.1.4. 2-(2-acetyl-5-methoxyphenoxy)-N-(o-tolyl)acetamide ***(3e)***. White solid, 44.54% yield, m. p.:146–147 °C, ^{1}H NMR (600 MHz, DMSO-d_6) δ 9.65 (s, 1H), 7.77 (d, J = 8.5 Hz, 1H), 7.45 (d, J = 7.8 Hz, 1H), 7.24 (d, J = 7.2 Hz, 1H), 7.19 (dt, J = 7.8, 4.0 Hz, 1H), 7.12 (t, J = 7.5 Hz, 1H), 6.71–6.63 (m, 2H), 4.90 (s, 2H), 3.84 (s, 3H), 2.58 (s, 3H), 2.22 (s, Hz, 3H). ^{13}C NMR (151 MHz, DMSO-d_6) δ 197.13, 166.56, 164.54, 159.45, 135.89, 132.94, 132.16, 130.83, 126.50, 126.00, 125.34, 120.82, 107.04, 100.19, 68.12, 56.14, 31.43, 18.10. HRMS (ESI): *m/z* $[M+Na]^+$ calcd for $C_{18}H_{19}NO_4Na$: 336.1206; found: 336.1207.

4.2.1.5. 2-(2-acetyl-5-methoxyphenoxy)-N-phenylacetamide ***(3f)***. White solid, 52.74% yield, m. p.:163–164 °C, ^{1}H NMR (600 MHz, DMSO-d_6) δ 10.27 (s, 1H), 7.81–7.76 (m, 1H), 7.68 (d, J = 7.9 Hz, 2H), 7.35 (t, J = 7.9 Hz, 2H), 7.10 (t, J = 7.4 Hz, 1H), 6.66 (dd, J = 6.7, 2.6 Hz, 2H), 4.85 (s, 2H), 3.83 (s, 3H), 2.60 (s, 3H). ^{13}C NMR (151 MHz, DMSO-d_6) δ 197.41, 166.48, 164.62, 159.47, 138.76, 133.09, 129.31 (2C), 124.19, 120.74, 119.75 (2C), 107.07, 100.36, 68.26, 56.15, 31.27. HRMS (ESI): *m/z* $[M+Na]^+$ calcd for $C_{17}H_{17}NO_4Na$: 322.1050; found: 22.1050.

4.2.1.6. 2-(2-acetyl-5-methoxyphenoxy)-N-(4-methoxyphenyl)acetamide ***(3g)***. White solid, 46.46% yield, m. p.:154–155 °C, ^{1}H NMR (600 MHz, DMSO-d_6) δ 10.18 (s, 1H), 7.87–7.70 (m, 1H), 7.65–7.54 (m, 2H), 6.94–6.87 (m, 2H), 6.66 (dd, J = 6.9, 2.3 Hz, 2H), 4.83 (s, 2H), 3.83 (s, 3H), 3.73 (s, 3H), 2.59 (s, 3H). ^{13}C NMR (151 MHz, DMSO-d_6) δ 197.43, 165.99, 164.62, 159.52, 156.06, 133.07, 131.90, 121.31 (2C), 120.75, 114.48(2C), 107.07, 100.35, 68.28, 56.14, 55.65, 31.29. HRMS (ESI): *m/z* $[M+Na]^+$ calcd for $C_{18}H_{19}NO_5Na$: 352.1155; found: 352.1156.

4.2.1.7. 2-(2-acetyl-5-methoxyphenoxy)-N-(2-fluorophenyl)acetamide ***(3h)***. White solid, 22.51% yield, m. p.:151–152 °C, ^{1}H NMR (600 MHz, DMSO-d_6) δ 10.00 (s, 1H), 7.90 (td, J = 7.6, 3.5 Hz, 1H), 7.75 (d, J = 8.7 Hz, 1H), 7.29 (ddd, J = 10.7, 6.1, 2.4 Hz, 1H), 7.20 (ddt, J = 10.0, 7.4, 3.8 Hz, 2H), 6.66 (d, J = 7.7 Hz, 2H), 4.94 (s, 2H), 3.83 (s, 3H), 2.58 (s, 3H). ^{13}C NMR (151 MHz, DMSO-d_6) δ 196.99, 166.89, 164.52, 159.45, 154.29 (d, $J_{C\text{-}F}$ = 245.5 Hz), 132.76, 126.31 (d, $J_{C\text{-}F}$ = 7.5 Hz), 125.76 (d, $J_{C\text{-}F}$ = 11.7 Hz), 124.87 (d, $J_{C\text{-}F}$ = 3.5 Hz), 124.74, 120.98, 116.01 (d, $J_{C\text{-}F}$ = 19.4 Hz), 107.14, 100.14, 68.01, 56.12, 31.48. HRMS (ESI): *m/z* $[M+Na]^+$ calcd for $C_{17}H_{16}FNO_4Na$: 340.0956; found: 340.0959.

4.2.1.8. 2-(2-acetyl-5-methoxyphenoxy)-N-(3-fluorophenyl)acetamide ***(3i)***. White solid, 41.89% yield, m. p.:157–158 °C, ^{1}H NMR (600 MHz, DMSO-d_6) δ 10.48 (s, 1H), 7.81–7.75 (m, 1H), 7.65 (dt, J = 11.4, 2.3 Hz, 1H), 7.44–7.35 (m, 2H), 6.93 (td, J = 8.0, 2.8 Hz, 1H), 6.67 (d, J = 7.1 Hz, 2H), 4.87 (s, 2H), 3.83 (s, 3H), 2.60 (s, 3H). ^{13}C NMR (151 MHz, DMSO-d_6) δ 197.47, 166.91, 164.63, 162.61 (d, $J_{C\text{-}F}$ = 241.8 Hz), 159.41, 140.46 (d, $J_{C\text{-}F}$ = 11.1 Hz), 131.00 (d, $J_{C\text{-}F}$ = 9.6 Hz), 133.09, 120.75, 115.50, 110.68 (d, $J_{C\text{-}F}$ = 21.0 Hz), 106.56 (d, $J_{C\text{-}F}$ = 26.1 Hz), 107.14, 100.40, 68.22, 56.16, 31.30. HRMS (ESI): *m/z* $[M+Na]^+$ calcd for $C_{17}H_{16}FNO_4Na$: 340.0956; found: 340.0957.

4.2.1.9. 2-(2-acetyl-5-methoxyphenoxy)-N-(4-fluorophenyl)acetamide ***(3j)***. White solid, 36.65% yield, m. p.:155–156 °C, ^{1}H NMR (600 MHz, DMSO-d_6) δ 10.36 (s, 1H), 7.81–7.75 (m, 1H), 7.70 (dd, J = 9.0, 4.9 Hz, 2H), 7.19 (t, J = 8.9 Hz, 2H), 6.70–6.62 (m, 2H), 4.85 (s, 2H), 3.83 (s, 3H), 2.59 (s, 3H). ^{13}C NMR (151 MHz, DMSO-d_6) δ 197.44, 166.44, 164.62, 159.46, 158.75 (d, $J_{C\text{-}F}$ = 240.3 Hz), 135.15 (d, $J_{C\text{-}F}$ = 2.5 Hz), 133.06, 121.59 (d, $J_{C\text{-}F}$ = 7.9 Hz, 2C), 120.80, 115.89 (d, $J_{C\text{-}F}$ = 22.4 Hz, 2C), 107.13, 100.41, 68.27, 56.15, 31.27. HRMS (ESI): m/z [M + Na]$^+$ calcd for $C_{17}H_{16}FNO_4Na$: 340.0956; found: 340.0958.

4.2.1.10. 2-(2-acetyl-5-methoxyphenoxy)-1-(4-methylpiperazin-1-yl) ethan-1-one ***(3k)***. oily liquid, 59.67% yield, ^{1}H NMR (600 MHz, DMSO-d_6) δ 7.65 (d, J = 8.7 Hz, 1H), 6.64–6.59 (m, 2H), 5.00 (s, 2H), 3.81 (s, 3H), 3.46 (t, J = 5.0 Hz, 4H), 2.58 (s, 3H), 2.30 (dt, J = 41.9, 5.0 Hz, 4H), 2.18 (s, 3H). ^{13}C NMR (151 MHz, DMSO-d_6) δ 197.11, 165.71, 164.43, 159.96, 132.10, 121.25, 106.51, 100.13, 66.65, 56.05, 55.06, 54.68, 46.07, 44.39, 41.62, 32.23. HRMS (ESI): m/z [M + Na]$^+$ calcd for $C_{16}H_{22}N_2O_4Na$: 329.1472; found: 329.1472.

4.2.1.11. 2-(2-acetyl-5-methoxyphenoxy)-1-morpholinoethan-1-one ***(3l)***. oily liquid, 55.52% yield, ^{1}H NMR (600 MHz, DMSO-d_6) δ 7.66 (d, J = 8.7 Hz, 1H), 6.64 (d, J = 2.3 Hz, 1H), 6.61 (dd, J = 8.7, 2.3 Hz, 1H), 5.02 (s, 2H), 3.81 (s, 3H), 3.60 (dt, J = 25.8, 4.7 Hz, 4H), 3.51–3.44 (m, 4H), 2.59 (s, 3H). ^{13}C NMR (151 MHz, DMSO-d_6) δ 197.13, 165.97, 164.44, 159.93, 132.12, 121.27, 106.47, 100.19, 66.56, 56.03, 45.04 (2C), 42.03 (2C), 32.21. HRMS (ESI): m/z [M + Na]$^+$ calcd for $C_{15}H_{19}NO_5Na$: 316.1155; found: 316.1158.

4.2.2. General procedure for synthesis of compounds ***6a-6m, 7a-7e***

K_2CO_3 (2.5 g, 18 mmol) was added to a stirring solution of the paeonol (2 g, 12 mmol), *tert*-butyl (2-bromoethyl)carbamate (5.35 g, 24 mmol) in DMF (15 mL) at 80 °C. Upon completion by TLC, the reaction mixture was cooled to room temperature, diluted with water, and extracted with EtOAc (3 × 50 mL). The combined organic fractions were washed with brine and dried over anhydrous sodium sulfate, filtered and concentrated by evaporation under reduced pressure. Residue was purified by flash chromatography gave intermediate **4** as white solid powder (2.23 g, yield 83%).

Intermediate **4** (2 g, 6.4 mmol) was dissolved in HCl/ethanol (1:1, 20 mL) and stirred at room temperature for 2 h. The solvent was then removed under reduced pressure to afford crude intermediate **5** (1.26 g, yield 90%) without further purification.

Intermediate **5** (100 mg, 0.479 mmol), benzoic acid (59 mg, 0.479 mmol) were dissolved in dichloromethane (5 mL). HOBT (90 mg, 0.669 mmol), EDCI (128 mg, 0.669 mmol) and Et_3N (215 μL, 1.338 mmol) were added at room temperature. The reaction mixture was stirred for overnight. After completion of the reaction, as indicated by TLC, the solvent was removed by rotary evaporation. Residue was purified by flash chromatography to gave compound **6a** (76 mg, 0.224 mmol, yield 51.08%) as white solid. ^{1}H NMR (400 MHz, DMSO-d_6) δ 8.71 (t, J = 5.3 Hz, 1H), 7.87–7.81 (m, 2H), 7.64 (d, J = 8.7 Hz, 1H), 7.56–7.43 (m, 3H), 6.69 (d, J = 2.2 Hz, 1H), 6.59 (dd, J = 8.7, 2.2 Hz, 1H), 4.28 (t, J = 5.6 Hz, 2H), 3.83 (s, 3H), 3.73 (q, J = 5.5 Hz, 2H), 2.47 (s, 3H). ^{13}C NMR (151 MHz, DMSO-d_6) δ 196.95, 167.07, 164.66, 160.47, 134.78, 132.14, 131.65, 128.72 (2C), 127.57 (2C), 120.99, 106.72, 99.36, 67.19, 56.05, 39.25, 32.30. HRMS (ESI): m/z [M + Na]$^+$ calcd for $C_{18}H_{19}NO_4Na$: 336.1206; found: 336.1209.

Following the similar procedures as for compound **6a** gave compounds **6b-6m**, **7a-7e**.

4.2.2.1. N-(2-(2-acetyl-5-methoxyphenoxy)ethyl)-2,4,5-trimethoxybenzamide ***(6b)***. White solid, 25.67% yield, m.p.: 133–134 °C. ^{1}H NMR (400 MHz, $CDCl_3$) δ 8.37 (t, J = 5.6 Hz, 1H), 7.65 (d, J = 8.7 Hz, 1H), 7.46 (s, 1H), 6.75 (s, 1H), 6.68 (d, J = 2.2 Hz, 1H), 6.59 (dd, J = 8.7, 2.2 Hz, 1H), 4.25 (t, J = 5.4 Hz, 2H), 3.89–3.81 (m, 9H), 3.76 (q, J = 5.5 Hz, 2H), 3.72 (s, 3H), 2.51 (d, J = 2.0 Hz, 3H).^{13}C NMR (151 MHz, DMSO-d_6) δ 196.81, 164.90, 164.69, 160.48, 153.02, 152.76, 142.98, 132.19, 120.84, 114.24, 112.94, 106.76, 99.34, 98.22, 67.68, 57.00, 56.38, 56.33, 56.05, 39.00, 32.23. HRMS (ESI): m/z [M + Na]$^+$ calcd for $C_{21}H_{25}NO_7Na$: 426.1523; found: 426.1520.

4.2.2.2. N-(2-(2-acetyl-5-methoxyphenoxy)ethyl)-3,4,5-trimethoxybenzamide ***(6c)***. White solid, 40.92% yield, m.p.: 149–150 °C. ^{1}H NMR (400 MHz, DMSO-d_6) δ 8.66 (t, J = 5.3 Hz, 1H), 7.65 (d, J = 8.7 Hz, 1H), 7.18 (s, 2H), 6.71 (d, J = 2.1 Hz, 1H), 6.60 (dd, J = 8.7, 2.1 Hz, 1H), 4.29 (t, J = 5.5 Hz, 2H), 3.83 (d, J = 5.4 Hz, 9H), 3.75–3.69 (m, 5H), 2.50 (s, 3H). ^{13}C NMR (151 MHz, DMSO-d_6) δ 197.04, 166.48, 164.64, 160.40, 153.00 (2C), 140.47, 132.17, 129.94, 121.07, 106.72, 105.24 (2C), 99.46, 67.15, 60.50, 56.43 (2C), 56.06, 39.30, 32.30. HRMS (ESI): m/z [M + Na]$^+$ calcd for $C_{21}H_{25}NO_7$ Na: 426.1523; found: 426.1519.

4.2.2.3. N-(2-(2-acetyl-5-methoxyphenoxy)ethyl)-4-(trifluoromethyl) benzamide ***(6d)***. White solid, 54.31% yield, m.p.: 154–155 °C. ^{1}H NMR (400 MHz, DMSO-d_6) δ 8.94 (t, J = 5.3 Hz, 1H), 8.04 (d, J = 8.1 Hz, 2H), 7.86 (d, J = 8.2 Hz, 2H), 7.64 (d, J = 8.7 Hz, 1H), 6.69 (d, J = 2.3 Hz, 1H), 6.60 (dd, J = 8.8, 2.3 Hz, 1H), 4.30 (t, J = 5.5 Hz, 2H), 3.83 (s, 3H), 3.75 (q, J = 5.4 Hz, 2H), 2.47 (s, 3H). ^{13}C NMR (151 MHz, DMSO-d_6) δ 196.91, 165.91, 164.66, 160.42, 138.51, 132.16, 131.61 (d, $J_{C\text{-}F}$ = 31.6 Hz), 128.50 (2C), 125.79 (d, $J_{C\text{-}F}$ = 3.6 Hz, 2C), 124.36 (q, $J_{C\text{-}F}$ = 272.5 Hz), 120.99, 106.72, 99.39, 67.06, 56.06, 39.42, 32.28. HRMS (ESI): m/z [M + Na]$^+$ calcd for $C_{19}H_{18}F_3NO_4$ Na: 404.1080; found: 404.1084.

4.2.2.4. N-(2-(2-acetyl-5-methoxyphenoxy)ethyl)-2,4-dichlorobenzamide ***(6e)***. White solid, 64.57% yield, m.p.: 125–127 °C. ^{1}H NMR (400 MHz, DMSO-d_6) δ 8.79 (t, J = 5.3 Hz, 1H), 7.67 (dd, J = 10.6, 5.3 Hz, 2H), 7.49 (dd, J = 8.2, 1.9 Hz, 1H), 7.42 (d, J = 8.2 Hz, 1H), 6.67 (d, J = 2.2 Hz, 1H), 6.60 (dd, J = 8.7, 2.2 Hz, 1H), 4.25 (t, J = 5.2 Hz, 2H), 3.83 (s, 3H), 3.70 (q, J = 5.2 Hz, 2H), 2.52 (d, J = 4.4 Hz, 3H). ^{13}C NMR (151 MHz, DMSO-d_6) δ 197.00, 166.18, 164.64, 160.44, 136.08, 134.95, 132.15, 131.58, 130.61, 129.57, 127.74, 121.00, 106.61, 99.34, 67.23, 56.07, 39.26, 32.51. HRMS (ESI): m/z [M + Na]$^+$ calcd for $C_{18}H_{17}Cl_2NO_4$ Na: 404.0427; found: 404.0431.

4.2.2.5. N-(2-(2-acetyl-5-methoxyphenoxy)ethyl)-2-chlorobenzamide ***(6f)***. White solid, 56.98% yield, m.p.: 111–112 °C. ^{1}H NMR (400 MHz, DMSO-d_6) δ 8.74 (t, J = 5.3 Hz, 1H), 7.67 (d, J = 8.7 Hz, 1H), 7.52–7.37 (m, 4H), 6.68 (d, J = 2.1 Hz, 1H), 6.61 (dd, J = 8.7, 2.1 Hz, 1H), 4.27 (t, J = 5.2 Hz, 2H), 3.84 (s, 3H), 3.71 (q, J = 5.2 Hz, 2H), 2.54 (s, 3H). ^{13}C NMR (151 MHz, DMSO-d_6) δ 197.02, 167.06, 164.64, 160.48, 137.28, 132.15, 131.19, 130.31, 130.03, 129.21, 127.49, 121.03, 106.61, 99.34, 67.27, 56.07, 39.22, 32.51. HRMS (ESI): m/z [M + Na]$^+$ calcd for $C_{18}H_{18}ClNO_4$ Na: 370.0817; found: 370.0820.

4.2.2.6. N-(2-(2-acetyl-5-methoxyphenoxy)ethyl)-4-methylbenzamide ***(6g)***. White solid, 46.40% yield, m.p.: 124–125 °C. ^{1}H NMR (400 MHz, DMSO-d_6) δ 8.63 (t, J = 5.2 Hz, 1H), 7.76 (d, J = 8.1 Hz, 2H), 7.65 (d, J = 8.7 Hz, 1H), 7.27 (d, J = 8.1 Hz, 2H), 6.69 (d, J = 2.1 Hz, 1H), 6.60 (dd, J = 8.7, 2.1 Hz, 1H), 4.28 (t, J = 5.6 Hz, 2H), 3.83 (s, 3H), 3.72 (q, J = 5.5 Hz, 2H), 2.47 (s, 3H), 2.35 (s, 3H). ^{13}C NMR (151 MHz, DMSO-d_6) δ 196.95, 166.92, 164.66, 160.48, 141.52, 132.13, 131.96, 129.24 (2C), 127.59 (2C), 120.98, 106.73, 99.35, 67.20, 56.06, 39.18, 32.31, 21.37. HRMS (ESI): m/z [M + H]$^+$ calcd for $C_{19}H_{22}NO_4$: 350.1363; found: 350.1367.

4.2.2.7. N-(2-(2-acetyl-5-methoxyphenoxy)ethyl)-4-nitrobenzamide ***(6h)***. White solid, 32.69% yield, m.p.: 162–164 °C. ^{1}H NMR (400 MHz, DMSO-d_6) δ 9.05 (t, J = 5.2 Hz, 1H), 8.33 (d, J = 8.7 Hz, 2H), 8.08 (d, J = 8.7 Hz, 2H), 7.65 (d, J = 8.7 Hz, 1H), 6.70 (d, J = 2.1 Hz, 1H), 6.60 (dd, J = 8.7, 2.1 Hz, 1H), 4.31 (t, J = 5.4 Hz, 2H), 3.83 (s, 3H),

3.77 (q, J = 5.3 Hz, 2H), 2.47 (s, 3H). ^{13}C NMR (151 MHz, DMSO-d_6) δ 196.90, 165.45, 164.66, 160.40, 149.51, 140.37, 132.16, 129.10 (2C), 123.99 (2C), 121.00, 106.74, 99.41, 67.02, 56.08, 39.52, 32.28. HRMS (ESI): m/z $[M+Na]^+$ calcd for $C_{18}H_{18}N_2O_6$ Na: 381.1057; found: 381.1056.

4.2.2.8. N-(2-(2-acetyl-5-methoxyphenoxy)ethyl)-3-chloro-4-fluorobenzamide ***(6i)***. White solid, 32.07% yield, m.p.: 135–136 °C. ^{1}H NMR (400 MHz, DMSO-d_6) δ 8.84 (t, J = 5.1 Hz, 1H), 8.06 (dd, J = 7.2, 2.1 Hz, 1H), 7.88 (ddd, J = 8.3, 4.7, 2.1 Hz, 1H), 7.65 (d, J = 8.7 Hz, 1H), 7.54 (t, J = 8.9 Hz, 1H), 6.69 (d, J = 2.1 Hz, 1H), 6.60 (dd, J = 8.7, 2.1 Hz, 1H), 4.29 (t, J = 5.5 Hz, 2H), 3.83 (s, 3H), 3.73 (q, J = 5.4 Hz, 2H), 2.47 (s, 3H). ^{13}C NMR (151 MHz, DMSO-d_6) δ 196.90, 164.72 (d, $J_{C\text{-}F}$ = 20.5 Hz), 160.41, 160.19, 158.53, 132.33, 132.16, 130.06, 128.87 (d, $J_{C\text{-}F}$ = 8.2 Hz), 120.99, 120.06 (d, $J_{C\text{-}F}$ = 18.1 Hz), 117.41 (d, $J_{C\text{-}F}$ = 21.1 Hz), 106.72, 99.39, 67.04, 56.06, 39.45, 32.28. HRMS (ESI): m/z $[M+Na]^+$ calcd for $C_{18}H_{17}ClFNO_4Na$: 388.0722; found: 388.0726.

4.2.2.9. N-(2-(2-acetyl-5-methoxyphenoxy)ethyl) cyclopropanecarboxamide ***(6j)***. White solid, 36.29% yield, m.p.: 138–140 °C. ^{1}H NMR (400 MHz, DMSO-d_6) δ 8.32 (t, J = 5.2 Hz, 1H), 7.66 (d, J = 8.7 Hz, 1H), 6.65 (d, J = 2.1 Hz, 1H), 6.60 (dd, J = 8.7, 2.1 Hz, 1H), 4.14 (t, J = 5.4 Hz, 2H), 3.83 (s, 3H), 3.53 (q, J = 5.4 Hz, 2H), 2.51 (s, 3H), 1.62–1.53 (m, 1H), 0.71–0.61 (m, 4H). ^{13}C NMR (151 MHz, DMSO-d_6) δ 196.97, 173.35, 164.66, 160.48, 132.14, 120.93, 106.73, 99.33, 67.63, 56.06, 38.67, 32.39, 13.98, 6.65(2C). HRMS (ESI): m/z $[M+Na]^+$ calcd for $C_{15}H_{19}NO_4Na$: 300.1206; found: 300.1209.

4.2.2.10. N-(2-(2-acetyl-5-methoxyphenoxy)ethyl)furan-2-carboxamide ***(6k)***. White solid, 55.18% yield, m.p.: 125–127 °C. ^{1}H NMR (400 MHz, DMSO-d_6) δ 8.59 (t, J = 5.5 Hz, 1H), 7.86–7.81 (m, 1H), 7.64 (d, J = 8.7 Hz, 1H), 7.11 (d, J = 3.5 Hz, 1H), 6.67 (d, J = 2.1 Hz, 1H), 6.60 (ddd, J = 10.9, 6.1, 2.0 Hz, 2H), 4.24 (t, J = 5.6 Hz, 2H), 3.82 (s, 3H), 3.72–3.63 (m, 2H), 2.46 (s, 3H). ^{13}C NMR (151 MHz, DMSO-d_6) δ 196.96, 164.65, 160.39, 158.49, 148.27, 145.46, 132.14, 120.98, 113.88, 112.26, 106.78, 99.34, 67.13, 56.05, 38.42, 32.27. HRMS (ESI): m/z $[M+Na]^+$ calcd for $C_{16}H_{17}NO_5$ Na: 326.0999; found: 326.0998.

4.2.2.11. N-(2-(2-acetyl-5-methoxyphenoxy)ethyl)nicotinamide ***(6l)***. White solid, 24.03% yield, m.p.: 108–110 °C. ^{1}H NMR (400 MHz, DMSO-d_6) δ 9.00 (d, J = 1.8 Hz, 1H), 8.92 (t, J = 5.1 Hz, 1H), 8.71 (d, J = 3.8 Hz, 1H), 8.18 (dd, J = 7.9, 1.6 Hz, 1H), 7.64 (d, J = 8.7 Hz, 1H), 7.51 (dd, J = 7.9, 4.8 Hz, 1H), 6.69 (d, J = 2.1 Hz, 1H), 6.60 (dd, J = 8.7, 2.1 Hz, 1H), 4.30 (t, J = 5.4 Hz, 2H), 3.83 (s, 3H), 3.75 (q, J = 5.4 Hz, 2H), 2.47 (s, 3H). ^{13}C NMR (151 MHz, $CDCl_3$) δ 197.57, 165.57, 164.36, 159.80, 151.89, 148.44, 135.29, 132.83, 129.88, 123.30, 121.42, 106.03, 100.83, 68.12, 55.53, 39.27, 30.10. HRMS (ESI): m/z $[M+Na]^+$ calcd for $C_{17}H_{18}N_2O_4$ Na: 337.1159; found: 337.1162.

4.2.2.12. N-(2-(2-acetyl-5-methoxyphenoxy)ethyl)furan-3-carboxamide ***(6m)***. White solid, 52.42% yield, m.p.: 125–126 °C. ^{1}H NMR (400 MHz, DMSO-d_6) δ 8.41 (t, J = 5.3 Hz, 1H), 8.18 (s, 1H), 7.73 (t, J = 1.6 Hz, 1H), 7.65 (d, J = 8.7 Hz, 1H), 6.85 (d, J = 1.6 Hz, 1H), 6.69 (d, J = 2.2 Hz, 1H), 6.60 (dd, J = 8.7, 2.2 Hz, 1H), 4.25 (t, J = 5.6 Hz, 2H), 3.83 (s, 3H), 3.67 (q, J = 5.5 Hz, 2H), 2.47 (s, 3H). ^{13}C NMR (151 MHz, DMSO-d_6) δ 196.98, 164.65, 162.42, 160.41, 145.54, 144.45, 132.15, 123.10, 121.00, 109.30, 106.77, 99.38, 67.19, 56.06, 38.65, 32.28. HRMS (ESI): m/z $[M+H]^+$ calcd for $C_{16}H_{18}NO_5$: 304.1179; found: 304.1178.

4.2.2.13. (E)-N-(2-(2-acetyl-5-methoxyphenoxy)ethyl)-3-(3,4,5-trimethoxyphenyl)acrylamide ***(7a)***. White solid, 48.47% yield, m.p.: 125–127 °C. ^{1}H NMR (400 MHz, $CDCl_3$) δ 7.75 (d, J = 8.7 Hz, 1H), 7.56 (d, J = 15.6 Hz, 1H), 6.93 (d, J = 4.4 Hz, 1H), 6.72 (s, 2H), 6.53 (dd, J = 8.8, 2.3 Hz, 1H), 6.43 (dd, J = 8.9, 6.5 Hz, 2H), 4.18 (t, J = 5.1 Hz, 2H), 3.88–3.81 (m, 14H), 2.58 (s, 3H). ^{13}C NMR (151 MHz, $CDCl_3$) δ 197.62, 166.14, 164.44, 159.87, 153.36 (2C), 141.09, 139.68, 132.80, 130.40, 121.23, 119.99, 105.89, 105.11 (2C), 99.99, 67.91, 60.88, 56.12(2C), 55.54, 38.92, 30.85. HRMS (ESI): m/z $[M+Na]^+$ calcd for $C_{23}H_{27}NO_7Na$: 452.1680; found: 452.1680.

4.2.2.14. N-(2-(2-acetyl-5-methoxyphenoxy)ethyl)cinnamamide ***(7b)***. White solid, 44.02% yield, m.p.: 129–130 °C. ^{1}H NMR (400 MHz, $CDCl_3$) δ 7.76 (d, J = 8.7 Hz, 1H), 7.65 (d, J = 15.7 Hz, 1H), 7.50 (dd, J = 7.3, 2.2 Hz, 2H), 7.38–7.32 (m, 3H), 7.00 (s, 1H), 6.54 (d, J = 1.6 Hz, 1H), 6.52–6.49 (m, 1H), 6.45 (d, J = 2.3 Hz, 1H), 4.19 (t, J = 5.2 Hz, 2H), 3.87–3.81 (m, 5H), 2.59 (s, 3H). ^{13}C NMR (151 MHz, $CDCl_3$) δ 197.56, 166.16, 164.41, 159.86, 141.17, 134.86, 132.79, 129.61, 128.74 (2C), 127.82 (2C), 121.31, 120.62, 105.95, 100.09, 67.97, 55.54, 38.91, 30.79. HRMS (ESI): m/z $[M+Na]^+$ calcd for $C_{20}H_{21}NO_4Na$: 362.1363; found: 362.1367.

4.2.2.15. (E)-N-(2-(2-acetyl-5-methoxyphenoxy)ethyl)-3-(4-nitrophenyl) acrylamide ***(7c)***. White solid, 30.75% yield, m.p.: 179–180 °C. ^{1}H NMR (400 MHz, DMSO-d_6) δ 8.53 (t, J = 5.3 Hz, 1H), 8.26 (d, J = 8.2 Hz, 2H), 7.84 (d, J = 8.4 Hz, 2H), 7.69–7.64 (m, 1H), 7.57 (d, J = 15.8 Hz, 1H), 6.87 (d, J = 15.8 Hz, 1H), 6.68 (d, J = 1.3 Hz, 1H), 6.63–6.58 (m, 1H), 4.23 (t, J = 5.2 Hz, 2H), 3.83 (s, 3H), 3.68 (dd, J = 10.4, 5.1 Hz, 2H), 2.51 (s, 3H). ^{13}C NMR (151 MHz, DMSO-d_6) δ 196.90, 165.10, 164.68, 160.43, 147.98, 141.91, 137.07, 132.17, 129.04(2C), 126.64, 124.53(2C), 120.92, 106.78, 99.33, 67.48, 56.09, 38.94, 32.40. HRMS (ESI): m/z $[M+Na]^+$ calcd for $C_{20}H_{20}N_2O_6Na$: 407.1214; found: 407.1216.

4.2.2.16. (E)-N-(2-(2-acetyl-5-methoxyphenoxy)ethyl)-3-(furan-2-yl) acrylamide ***(7d)***. White solid, 43.52% yield, m.p.: 105–107 °C. ^{1}H NMR (400 MHz, $CDCl_3$) δ 7.79 (d, J = 8.7 Hz, 1H), 7.47–7.41 (m, 2H), 6.83 (s, 1H), 6.57–6.53 (m, 2H), 6.48–6.44 (m, 2H), 6.41 (d, J = 15.4 Hz, 1H), 4.20 (t, J = 5.2 Hz, 2H), 3.87–3.82 (m, 5H), 2.60 (s, 3H). ^{13}C NMR (151 MHz, DMSO-d_6) δ 196.93, 165.62, 164.67, 160.46, 151.35, 145.19, 132.15, 126.72, 120.92, 119.58, 114.26, 112.81, 106.78, 99.31, 67.55, 56.06, 38.83, 32.38. HRMS (ESI): m/z $[M+Na]^+$ calcd for $C_{18}H_{19}NO_5Na$: 352.1155; found: 352.1159.

4.2.2.17. (E)-N-(2-(2-acetyl-5-methoxyphenoxy)ethyl)-3-(3,5,6-trimethylpyrazin-2-yl)acrylamide ***(7e)***. White solid, 29.85% yield, m.p.: 105–107 °C. ^{1}H NMR (400 MHz, $CDCl_3$) δ 7.83 (d, J = 14.9 Hz, 1H), 7.78 (d, J = 8.7 Hz, 1H), 7.10 (d, J = 14.9 Hz, 1H), 6.82 (s, 1H), 6.53 (dd, J = 8.8, 2.3 Hz, 1H), 6.44 (d, J = 2.3 Hz, 1H), 4.19 (t, J = 5.2 Hz, 2H), 3.89–3.82 (m, 5H), 2.59 (d, J = 4.3 Hz, 6H), 2.49 (d, J = 5.8 Hz, 6H). ^{13}C NMR (151 MHz, $CDCl_3$) δ 197.37, 165.86, 164.41, 159.85, 152.01, 149.50, 148.84, 143.00, 135.59, 132.80, 125.45, 121.25, 105.89, 99.79, 67.77, 55.52, 39.03, 31.02, 21.88, 21.63, 20.70. HRMS (ESI): m/z $[M+Na]^+$ calcd for $C_{21}H_{25}N_3O_4Na$: 406.1737; found: 406.1742.

4.2.3. General procedure for synthesis of compounds ***10a-10e, 11a-11e***

K_2CO_3 (2.5 g, 18 mmol) was added to a stirring solution of the paeonol (2 g, 12 mmol) and 1-fluoro-4-nitrobenzene (2 g, 14.4 mmol) in DMSO (20 mL) at room temperature. The reaction mixture was stirred for overnight and monitored by TLC. Upon completion, the reaction mixture was diluted with water and extracted with EtOAc (3 × 50 mL). The combined organic fractions were washed with brine and dried over anhydrous sodium sulfate, filtered and concentrated by evaporation under reduced pressure. Residue was purified by flash chromatography to gave intermediate **8** as yellow oil liquid (2.96 g; yield 86%).

Intermediate **8** (2 g, 17.4 mmol) was dissolved in methanol (40 mL)

and 10% Pd-C (4% mmol) was added under H_2 atmosphere. Monitored by TLC and upon completion, the reaction mixture was filtered and removed solvent by evaporation under reduced pressure, obtained crude intermediate **9** as yellow solid without further purification.

P-nitrobenzoic acid (65 mg, 0.39 mmol), oxalyl chloride (100 μL, 1.17 mmol) and catalytic DMF were dissolved in DCM (5 mL), and the mixture was stirred at 25 ˚C for 2 h. Then the mixture was concentrated under vacuum and directly used in next step without any further purification. The obtained corresponding acyl chloride was dissolved in DCM (2 mL) and the solution was added to the mixture of intermediate **9** (100 mg, 0.39 mmol) and Et_3N (192 μL, 1.2 mmol) in DCM (6 mL) at 0 ˚C. The solution was allowed to stir at 0 ˚C to room temperature for overnight. Reaction mixture was washed with brine. Organic solvent was dried over anhydrous sodium sulfate, filtrated, concentrated by evaporation under reduced pressure. Residue was purified by flash chromatography to gave compound **10a** (68 mg, 0.168 mmol, yield 43.12%). ^{1}H NMR (600 MHz, $CDCl_3$) δ 8.33 (d, J = 8.6 Hz, 2H), 8.11–8.08 (m, 1H), 8.06 (d, J = 8.6 Hz, 2H), 7.90 (d, J = 8.9 Hz, 1H), 7.66 (d, J = 8.7 Hz, 2H), 7.05 (d, J = 8.8 Hz, 2H), 6.73–6.69 (m, 1H), 6.38 (d, J = 2.2 Hz, 1H), 3.77 (s, 3H), 2.60 (s, 3H). ^{13}C NMR (151 MHz, $CDCl_3$) δ 196.82, 164.26, 158.29, 153.37, 149.87, 140.28, 133.24, 132.60, 128.21 (2C), 124.00 (2C), 123.17, 122.39 (2C), 119.54 (2C), 109.99, 109.43, 104.62, 55.58, 31.29. HRMS (ESI): m/z $[M+Na]^+$ calcd for $C_{22}H_{18}N_2O_6Na$: 429.1057; found: 429.1055.

Following the similar procedures as for compound **10a** gave compounds **10b-10e, 11a-11e**.

4.2.3.1. N-(4-(2-acetyl-5-methoxyphenoxy)phenyl)-4-fluorobenzamide ***(10b)***. White solid, 39.16% yield, m.p.: 154–155 ˚C. ^{1}H NMR (600 MHz, $CDCl_3$) δ 8.03 (s, 1H), 7.91–7.88 (m, 3H), 7.64 (d, J = 8.9 Hz, 2H), 7.15 (t, J = 8.6 Hz, 2H), 7.03 (d, J = 8.9 Hz, 2H), 6.68 (dd, J = 8.8, 2.4 Hz, 1H), 6.36 (d, J = 2.3 Hz, 1H), 3.75 (s, 3H), 2.60 (s, 3H). ^{13}C NMR (151 MHz, $CDCl_3$) δ 196.99, δ 164.93 (d, $J_{C\text{-}F}$ = 252.8 Hz), 164.69, 164.28, 158.63, 152.70, 134.01, 132.52, 130.94 (d, $J_{C\text{-}F}$ = 3.0 Hz), 129.42 (d, $J_{C\text{-}F}$ = 8.9 Hz, 2C), 122.98, 122.29 (2C), 119.58 (2C), 115.79 (d, $J_{C\text{-}F}$ = 22.0 Hz, 2C), 109.28, 104.29, 55.55, 31.33. HRMS (ESI): m/z $[M+Na]^+$ calcd for $C_{22}H_{18}FNO_4Na$: 402.1112; found: 402.1111.

4.2.3.2. N-(4-(2-acetyl-5-methoxyphenoxy)phenyl)benzamide ***(10c)***. White solid, 30.24% yield, m.p.: 140–141 ˚C. ^{1}H NMR (600 MHz, $CDCl_3$) δ 7.92–7.86 (m, 3H), 7.66 (d, J = 8.9 Hz, 2H), 7.58–7.46 (m, 3H), 7.05 (dt, J = 5.0, 3.1 Hz, 2H), 6.70–6.67 (m, 1H), 6.37 (d, J = 2.3 Hz, 1H), 3.75 (d, J = 1.3 Hz, 3H), 2.61 (d, J = 1.5 Hz, 3H). ^{13}C NMR (151 MHz, DMSO-d_6) δ 196.23, 165.86, 164.29, 158.59, 152.00, 135.84, 135.35, 132.56, 131.95, 128.80, 128.04, 122.93, 122.61, 119.47, 109.86, 104.65, 56.15, 31.47. HRMS (ESI): m/z $[M+Na]^+$ calcd for $C_{22}H_{19}NO_4Na$: 384.1206; found: 384.1209.

4.2.3.3. N-(4-(2-acetyl-5-methoxyphenoxy)phenyl)furan-2-carboxamide ***(10d)***. White solid, 32.87% yield, m.p.: 108–109 ˚C. ^{1}H NMR (600 MHz, $CDCl_3$) δ 8.11 (s, 1H), 7.90 (dd, J = 8.7, 7.2 Hz, 1H), 7.66 (d, J = 8.7 Hz, 2H), 7.52–7.48 (m, 1H), 7.25–7.22 (m, 1H), 7.07–7.00 (m, 2H), 6.71–6.65 (m, 1H), 6.56 (ddd, J = 12.7, 3.5, 1.7 Hz, 1H), 6.36 (d, J = 2.3 Hz, 1H), 5.29 (d, J = 6.5 Hz, 1H), 3.77–3.70 (m, 3H), 2.61–2.59 (m, 3H). ^{13}C NMR (151 MHz, DMSO-d_6) δ 196.22, 164.28, 158.50, 156.57, 152.12, 147.97, 146.06, 135.13, 132.55, 122.96, 122.64 (2C), 119.44 (2C), 115.07, 112.54, 109.89, 104.74, 56.16, 31.45. HRMS (ESI): m/z $[M+Na]^+$ calcd for $C_{20}H_{17}NO_5Na$: 374.0999; found: 374.1002.

4.2.3.4. N-(4-(2-acetyl-5-methoxyphenoxy)phenyl)nicotinamide ***(10e)***. White solid, 30.79% yield, m.p.: 140–141 ˚C. ^{1}H NMR (600 MHz, $CDCl_3$) δ 9.11 (s, 1H), 8.77 (d, J = 3.8 Hz, 1H), 8.22 (d, J = 7.9 Hz, 1H), 8.11 (s, 1H), 7.91 (d, J = 8.9 Hz, 1H), 7.66 (d, J = 8.8 Hz, 2H), 7.45 (s, 1H), 7.05 (d, J = 8.9 Hz, 2H), 6.70 (dd, J = 8.9, 2.4 Hz, 1H), 6.37 (d, J = 2.3 Hz, 1H), 3.76 (s, 3H), 2.60 (s, 3H). ^{13}C NMR (151 MHz, DMSO-d_6) δ 196.24, 164.36, 164.29, 158.46, 152.52, 152.30, 149.06, 135.82, 135.43, 132.58, 130.96, 123.91, 122.97, 122.67 (2C), 119.48 (2C), 109.94, 104.76, 56.16, 31.44. HRMS (ESI): m/z $[M+Na]^+$ calcd for $C_{21}H_{18}N_2O_4Na$: 385.1159; found: 385.1156.

4.2.3.5. (E)-N-(4-(2-acetyl-5-methoxyphenoxy)phenyl)-3-(3,4,5-trimethoxyphenyl)acrylamide ***(11a)***. White solid, 49.35% yield, m.p.: 76–78 ˚C. ^{1}H NMR (400 MHz, $CDCl_3$) δ 7.91 (d, J = 8.8 Hz, 1H), 7.80 (s, 1H), 7.66 (dd, J = 11.9, 8.6 Hz, 3H), 7.03–6.99 (m, 2H), 6.75 (s, 2H), 6.67 (dd, J = 8.9, 2.4 Hz, 1H), 6.52 (d, J = 15.4 Hz, 1H), 6.34 (d, J = 2.4 Hz, 1H), 3.87 (d, J = 2.6 Hz, 3H), 3.86 (s, 6H), 3.74 (s, 3H), 2.61 (s, 3H). ^{13}C NMR (151 MHz, DMSO-d_6) δ 196.25, 164.28, 163.92, 158.68, 153.56 (2C), 151.61, 140.75, 139.44, 136.11, 132.58, 130.72, 122.80, 121.87, 121.32(2C), 119.79 (2C), 109.73 (2C), 105.64, 104.52, 60.55, 56.36 (2C), 56.13, 31.52. HRMS (ESI): m/z $[M+Na]^+$ calcd for $C_{27}H_{27}NO_7Na$: 500.1680; found: 500.1680.

4.2.3.6. N-(4-(2-acetyl-5-methoxyphenoxy)phenyl)cinnamamide ***(11b)***. White solid, 42.97% yield, m.p.: 128–129 ˚C. ^{1}H NMR (600 MHz,$CDCl_3$) δ 8.20 (s, 1H), 7.91 (dd, J = 8.8, 1.2 Hz, 1H), 7.75 (d, J = 15.5 Hz, 1H), 7.69 (d, J = 7.9 Hz, 2H), 7.50–7.44 (m, 2H), 7.37–7.30 (m, 3H), 7.02–6.97 (m, 2H), 6.66 (d, J = 8.9 Hz, 1H), 6.63 (dd, J = 15.5, 1.1 Hz, 1H), 6.33 (s, 1H), 3.72 (s, 3H), 2.61 (s, 3H). ^{13}C NMR (151 MHz, DMSO-d_6) δ 196.25, 164.28, 163.84, 158.65, 151.69, 140.58, 136.00, 135.16, 132.58, 130.21, 129.45 (2C), 128.15 (2C), 122.81, 122.62, 121.41 (2C), 119.77 (2C), 109.78, 104.56, 56.14, 31.52. HRMS (ESI): m/z $[M+Na]^+$ calcd for $C_{24}H_{21}NO_4Na$: 410.1363; found: 410.1366.

4.2.3.7. (E)-N-(4-(2-acetyl-5-methoxyphenoxy)phenyl)-3-(4-nitrophenyl) acrylamide ***(11c)***. White solid, 37.72% yield, m.p.: 186–187 ˚C. ^{1}H NMR (600 MHz, DMSO-d_6) δ 10.43 (s, 1H), 8.29 (d, J = 8.8 Hz, 2H), 7.89 (d, J = 8.8 Hz, 2H), 7.80 (d, J = 8.8 Hz, 1H), 7.76 (d, J = 8.9 Hz, 2H), 7.70 (d, J = 15.7 Hz, 1H), 7.12–7.07 (m, 2H), 7.00 (d, J = 15.8 Hz, 1H), 6.82 (dd, J = 8.9, 2.4 Hz, 1H), 6.38 (d, J = 2.4 Hz, 1H), 3.74 (s, 3H), 2.51 (s, 3H). ^{13}C NMR (151 MHz, DMSO-d_6) δ 196.23, 164.28, 163.12, 158.53, 151.97, 148.11, 141.73, 138.12, 135.70, 132.59, 129.19 (2C), 126.93, 124.60 (2C), 122.86, 121.52 (2C), 119.74 (2C), 109.86, 104.68, 56.15, 31.50. HRMS (ESI): m/z $[M+Na]^+$ calcd for $C_{24}H_{20}N_2O_6Na$: 455.1214; found: 455.1211.

4.2.3.8. (E)-N-(4-(2-acetyl-5-methoxyphenoxy)phenyl)-3-(furan-2-yl) acrylamide ***(11d)***. White solid, 50.17% yield, m.p.: 134–136 ˚C. ^{1}H NMR (400 MHz, $CDCl_3$ δ 7.91 (d, J = 8.8 Hz, 1H), 7.77 (s, 1H), 7.64 (d, J = 8.5 Hz, 2H), 7.52 (d, J = 15.2 Hz, 1H), 7.44 (d, J = 1.5 Hz, 1H), 7.03–6.98 (m, 2H), 6.67 (dd, J = 8.8, 2.4 Hz, 1H), 6.58 (d, J = 3.4 Hz, 1H), 6.52–6.44 (m, 2H), 6.33 (d, J = 2.3 Hz, 1H), 3.73 (s, 3H), 2.61 (s, 3H). ^{13}C NMR (151 MHz, DMSO-d_6) δ 196.25, 164.27, 163.72, 158.67, 151.64, 151.36, 145.56, 136.03, 132.56, 127.71, 122.80, 121.33 (2C), 119.78 (2C), 114.95, 112.99, 109.77 (2C), 104.50, 56.13, 31.51. HRMS (ESI): m/z $[M+Na]^+$ calcd for $C_{22}H_{19}NO_5Na$: 400.1155; found: 400.1155.

4.2.3.9. (E)-N-(4-(2-acetyl-5-methoxyphenoxy)phenyl)-3-(3,5,6-trimethyl-1,4-dihydropyrazin-2-yl)acrylamide ***(11e)***. White solid, 49.37% yield, m.p.: 222–224 ˚C. ^{1}H NMR (400 MHz, $CDCl_3$) δ 7.92 (dd, J = 11.7, 10.8 Hz, 2H), 7.82 (s, 1H), 7.66 (d, J = 8.8 Hz, 2H), 7.22 (d, J = 14.7 Hz, 1H), 7.04–6.99 (m, 2H), 6.67 (dd, J = 8.8, 2.4 Hz, 1H), 6.34 (d, J = 2.4 Hz, 1H), 3.74 (s, 3H), 2.61 (s, 6H), 2.51 (d, J = 10.2 Hz, 6H).^{13}C NMR (151 MHz, DMSO-d_6) δ 196.23, 164.28, 163.48, 158.61, 152.54, 151.80, 149.89, 148.86, 142.79, 135.97, 135.18, 132.57, 127.07, 122.84, 121.38 (2C), 119.74 (2C), 109.81, 104.58, 56.14, 31.49, 22.02, 21.76, 20.82. HRMS (ESI): m/z $[M+Na]^+$ calcd for $C_{25}H_{27}N_3O_4Na$: 454.1737; found: 454.1734.

4.3. Cell culture

Mouse peritoneal macrophages were obtained from the BeNa culture collection company. RAW264.7 cells were cultured in DMEM (Hyclone, USA) with 10% FBS (Biological Industries, Israel, 100 U/mL penicillin and 100 μg/mL streptomycin (Beyotime, China) at 37 ˚C in a humid environment containing 5% CO_2. All the cells used in the experiment are in the logarithmic growth stage, and the number of cells in the culture bottle is about 70%–80%.

4.4. Determination of NO release

RAW264.7 cells were seeded into 48well plates (NEST, China) at a density of 7×10^4 cells per well, and were used for experiments about 24 h later. RAW264.7 cells were pretreated with compounds (20 μM) for 1 h and incubated with LPS (0.5 μg/mL) for 24 h. Cell supernatant was collected for experiment. Measurement of NO production by Griess reagent assay (Beyotime, China).

4.5. Cell viability assay (MTT)

RAW264.7 cells were pretreated with all compounds (20 μM) for 24 h. RAW264.7 cells were seeded into 96 well plate, each well with 1×10^4 cells, and kept at 37 ˚C, 5% CO_2 for about 24 h. Discard the cell culture medium and add the compounds to treat the cell for 24 h. After MTT (sigma, USA, PBS solution at a concentration of 5 mg/mL) was added and incubated at 37 ˚C for 4 h, the medium containing MTT was removed , DMSO (150 μL) was added to each wells, Shaking for 10 min and the absorbance at 492 nm was measured by a microplate reader (MQX200, Bio-Tek, USA) [31].

4.6. Western blotting

RAW264.7 cells were seeded into 6-well plate with 4×10^6 cells or 2×10^6 cells per well and maintained at 37 ˚C in 5% CO_2 about 24 h. RAW264.7 cell were pretreated with compound **11a** (10, 5, 2.5 μM) for 1 h, incubated with LPS (0.5 μg/mL) for 0.5 h or 24 h. The cells were lysed in 400 uL RIPA cell lysis buffer (Contains PMSF and phosphatase inhibitors, Beyotime china) and incubated on ice for 30 min. High speed centrifugation for 10 min, proteins were run on 12% SDS-PAGE and then transferred to PVDF membrane (GE Healthcare, UK). The blotted membrane was incubated overnight at 4 ˚C with a specific primary antibody p-iκB, iNOS (CST, USA), iκB, COX-2 (abcam, USA), ERK, p-ERK, P38, p-P38, JNK, p-JNK (Immunoway, USA) The membranes were washed in TBST (Beyotime, China), incubated with a 1:5000 dilution of HRP-conjugated secondary antibody (ZSGB-BIO, China) for 1 h at room temperature.

4.7. In vivo experiment

The 50 male rats weighing 140–160 g were purchased from Animal Department of Anhui Medical University. All animal protocols were approved by the Ethics Committee in Animal Experimentation at Anhui Medical University (Hefei, China) following the guidelines for Care and Use of Laboratory Animals. After one-week acclimatization, mice were randomly divided into five groups on average, including the control group, AA group, Sinomenine (80 mg/kg), compound **11a** (40 mg/kg) and compound **11a** (80 mg/kg). Complete Freund's adjuvant consists of incomplete Freund's adjuvant (sigma, USA) and inactivated BCG vaccine (China) (10 mg/mL). Rat was induced by a single intradermal injection of 0.1 mL CFA into the right hind paw. Rats in the normal group were given the same amount of normal saline. All rats received intragastrical administration. At the end of the experiment, all rats were anesthetized and executed. The ankle joint was immediately removed, fixed in 4% neutral buffered polyformaldehyde solution, and then decalcified in 10% EDTA. After decalcification, the tissue was dehydrated according to gradient ethanol series, embedded in paraffin, cut into 4 mm thick. The sections were stained with hematoxylin and eosin (HE) for histopathological examination. Histological images were obtained using the 3DHISTECH's Slide Converter (3DHISTECH, Hungary).

4.8. Statistical analysis

The data were expressed as mean ± SEM and analyzed statistically by analysis of variance (ANOVE). $p < 0.05$ was considered statistically significant. Data were expressed as mean ± SEM and analyzed using GraphPad Prism version 6.0 (GraphPad Software, USA). All experiment data were repeated at least three times.

Declaration of Competing Interest

The authors declare that they have no known competing financial interests or personal relationships that could have appeared to influence the work reported in this paper.

Acknowledgment

This work was supported by the National Natural Science Funding of China (21977001 and 21572003).

Appendix A. Supplementary material

The following files are available free. ^{1}H NMR and ^{13}C NMR spectra and HRMS of all compounds.

Supplementary data to this article can be found online at https://doi.org/10.1016/j.bioorg.2020.103735.

References

[1] T.C. Chou, Anti-inflammatory and analgesic effects of paeonol in carrageenan-evoked thermal hyperalgesia, Br. J. Pharmacol. 139 (2003) 1146–1152.
[2] L. Zhang, D.C. Li, L.F. Liu, Paeonol: pharmacological effects and mechanisms of action, Int. Immunopharmacol. 72 (2019) 413–421.
[3] L. Zhang, L. Tao, T. Shi, F. Zhang, X. Sheng, Y. Cao, S. Zheng, A. Wang, W. Qian, L. Jiang, Y. Lu, Paeonol inhibits B16F10 melanoma metastasis in vitro and in vivo via disrupting proinflammatory cytokines-mediated NF-kappaB and STAT3 pathways, IUBMB Life 67 (2015) 778–788.
[4] Z.K. Lyu, C.L. Li, Y. Jin, Y.Z. Liu, X. Zhang, F. Zhang, L.N. Ning, E.S. Liang, M. Ma, W. Gao, M.X. Zhang, D.S. Liu, Paeonol exerts potential activities to inhibit the growth, migration and invasion of human gastric cancer BGC823 cells via down-regulating MMP2 and MMP9, Mol. Med. Rep. 16 (2017) 7513–7519.
[5] T.J. Huang, H. Chuang, Y.C. Liang, H.H. Lin, J.C. Horng, Y.C. Kuo, C.W. Chen, F.Y. Tsai, S.C. Yen, S.C. Chou, M.H. Hsu, Design, synthesis, and bioevaluation of paeonol derivatives as potential anti-HBV agents, Eur. J. Med. Chem. 90 (2015) 428–435.
[6] G.B. Park, D. Kim, MicroRNA-503-5p inhibits the CD97-mediated JAK2/STAT3 pathway in metastatic or paclitaxel-resistant ovarian cancer cells, Neoplasia 21 (2019) 206–215.
[7] C.H. Lau, C.M. Chan, Y.W. Chan, K.M. Lau, T.W. Lau, F.C. Lam, W.T. Law, C.T. Che, P.C. Leung, K.P. Fung, Y.Y. Ho, C.B. Lau, Pharmacological investigations of the anti-diabetic effect of Cortex Moutan and its active component paeonol, Phytomed. Int. J. Phytother. Phytopharm. 14 (2007) 778–784.
[8] B. Chen, M. Ning, G. Yang, Effect of paeonol on antioxidant and immune regulatory activity in hepatocellular carcinoma rats, Molecules 17 (2012) 4672–4683.
[9] P. Kirsch, A.M. Hartman, A.K.H. Hirsch, M. Empting, Concepts and core principles of fragment-based drug design, Molecules 24 (2019).
[10] J.B. Shi, L.Z. Chen, B.S. Wang, X. Huang, M.M. Jiao, M.M. Liu, W.J. Tang, X.H. Liu, Novel pyrazolo[4,3-*d*]pyrimidine as potent and orally active inducible nitric oxide synthase (iNOS) dimerization inhibitor with efficacy in rheumatoid arthritis mouse model, J. Med. Chem. 62 (2019) 4013–4031.
[11] R. Zhou, X. Wu, Z. Wang, J. Ge, F. Chen, Interleukin-6 enhances acid-induced apoptosis via upregulating acid-sensing ion channel 1a expression and function in rat articular chondrocytes, Int. Immunopharmacol. 29 (2015) 748–760.
[12] H. Marotte, E. Gineyts, P. Miossec, P.D. Delmas, Effects of infliximab therapy on biological markers of synovium activity and cartilage breakdown in patients with rheumatoid arthritis, Ann. Rheum. Dis. 68 (2009) 1197–1200.
[13] B. Bartok, G.S. Firestein, Fibroblast-like synoviocytes: key effector cells in rheumatoid arthritis, Immunol. Rev. 233 (2010) 233–255.
[14] D. Kesharwani, R. Paliwal, T. Satapathy, S. Das Paul, Rheumatiod arthritis: an updated overview of latest therapy and drug delivery, J. Pharmacop. 22 (2019)

210–224.
[15] K.F. Zhai, H. Duan, L. Luo, W.G. Cao, F.K. Han, L.L. Shan, X.M. Fang, Protective effects of paeonol on inflammatory response in IL-1beta-induced human fibroblast-like synoviocytes and rheumatoid arthritis progression via modulating NF-kappaB pathway, Inflammopharmacology (2017).
[16] Y. Lou, C. Wang, Q. Tang, W. Zheng, Z. Feng, X. Yu, X. Guo, J. Wang, Paeonol inhibits IL-1beta-induced inflammation via PI3K/Akt/NF-kappaB pathways in vivo and vitro studies, Inflammation 40 (2017) 1698–1706.
[17] Y. Tang, W. Huang, Q. Song, X. Zheng, R. He, J. Liu, Paeonol ameliorates ovalbumin-induced asthma through the inhibition of TLR4/NF-kappaB and MAPK signaling, Evid. Based Complem. Alternat. Med. 2018 (2018) 3063145.
[18] S.W. Himaya, B. Ryu, Z.J. Qian, S.K. Kim, Paeonol from Hippocampus kuda Bleeler suppressed the neuro-inflammatory responses in vitro via NF-kappaB and MAPK signaling pathways, Toxicol. In Vitro 26 (2012) 878–887.
[19] L. Huang, B. Zhang, Y. Yang, X. Gong, Z. Chen, Z. Wang, P. Zhang, Q. Zhang, Synthesis and anti-inflammatory activity of paeonol analogues in the murine model of complete Freund's adjuvant induced arthritis, Bioorg. Med. Chem. Lett. 26 (2016) 5218–5221.
[20] M. Catarro, J.L. Serrano, S.S. Ramos, S. Silvestre, P. Almeida, Nimesulide analogues: From anti-inflammatory to antitumor agents, Bioorg. Chem. 88 (2019) 102966.
[21] I. Nugrahani, D. Utami, Y.P. Nugraha, H. Uekusa, R. Hasianna, A.A. Darusman, Cocrystal construction between the ethyl ester with parent drug of diclofenac: structural, stability, and anti-inflammatory study, Heliyon 5 (2019) e02946.
[22] W.X. Zhang, H. Wang, H.R. Cui, W.B. Guo, F. Zhou, D.S. Cai, B. Xu, X.H. Jia, X.M. Huang, Y.Q. Yang, H.S. Chen, J.C. Qi, P.L. Wang, H.M. Lei, Design, synthesis and biological evaluation of cinnamic acid derivatives with synergetic neuroprotection and angiogenesis effect, Eur. J. Med. Chem. 183 (2019) 111695.
[23] M.G. Brasca, S. Mantegani, N. Amboldi, S. Bindi, D. Caronni, E. Casale, W. Ceccarelli, N. Colombo, A. De Ponti, D. Donati, A. Ermoli, G. Fachin, E.R. Felder, R.D. Ferguson, C. Fiorelli, M. Guanci, A. Isacchi, E. Pesenti, P. Polucci, L. Riceputi, F. Sola, C. Visco, F. Zuccotto, G. Fogliatto, Discovery of NMS-E973 as novel, selective and potent inhibitor of heat shock protein 90 (Hsp90), Bioorg. Med. Chem. 21 (2013) 7047–7063.
[24] M.-L. Tang, C. Zhong, Z.-Y. Liu, P. Peng, X.-H. Liu, X. Sun, Discovery of novel sesquistilbene indanone analogues as potent anti-inflammatory agents, Eur. J. Med. Chem. 113 (2016) 63–74.
[25] G. Nagy, J.M. Clark, E.I. Buzas, C.L. Gorman, A.P. Cope, Nitric oxide, chronic inflammation and autoimmunity, Immunol. Lett. 111 (2007) 1–5.
[26] L.D. Sun, F. Wang, F. Dai, Y.H. Wang, D. Lin, B. Zhou, Development and mechanism investigation of a new piperlongumine derivative as a potent anti-inflammatory agent, Biochem. Pharmacol. 95 (2015) 156–169.
[27] Y.S. Kim, C.B. Ahn, J.Y. Je, Anti-inflammatory action of high molecular weight Mytilus edulis hydrolysates fraction in LPS-induced RAW264.7 macrophage via NF-kappaB and MAPK pathways, Food Chem. 202 (2016) 9–14.
[28] H.Y. Zhou, E.M. Shin, L.Y. Guo, U.J. Youn, K. Bae, S.S. Kang, L.B. Zou, Y.S. Kim, Anti-inflammatory activity of 4-methoxyhonokiol is a function of the inhibition of iNOS and COX-2 expression in RAW 264.7 macrophages via NF-kappaB, JNK and p38 MAPK inactivation, Eur. J. Pharmacol. 586 (2008) 340–349.
[29] Z. Yuan, F.B. Matias, J. Wu, Z. Liang, Z. Sun, Koumine attenuates lipopolysaccaride-stimulated inflammation in RAW264.7 macrophages, coincidentally associated with inhibition of NF-kappaB, ERK and p38 pathways, Int. J. Mol. Sci. 17 (2016) 430.
[30] Y. Dondelinger, S. Jouan-Lanhouet, T. Divert, E. Theatre, J. Bertin, P.J. Gough, P. Giansanti, A.J. Heck, E. Dejardin, P. Vandenabeele, M.J. Bertrand, NF-kappaB-independent role of IKKalpha/IKKbeta in preventing RIPK1 kinase-dependent apoptotic and necroptotic cell death during TNF signaling, Mol. Cell 60 (2015) 63–76.
[31] K.H. Tse, K.B.S. Chow, W.K. Leung, Y.H. Wong, H. Wise, Lipopolysaccharide differentially modulates expression of cytokines and cyclooxygenases in dorsal root ganglion cells via Toll-like receptor-4 dependent pathways, Neuroscience 267 (2014) 241–251.
[32] X. Kuang, Y. Huang, H.F. Gu, X.Y. Zu, W.Y. Zou, Z.B. Song, Q.L. Guo, Effects of intrathecal epigallocatechin gallate, an inhibitor of Toll-like receptor 4, on chronic neuropathic pain in rats, Eur. J. Pharmacol. 676 (2012) 51–56.